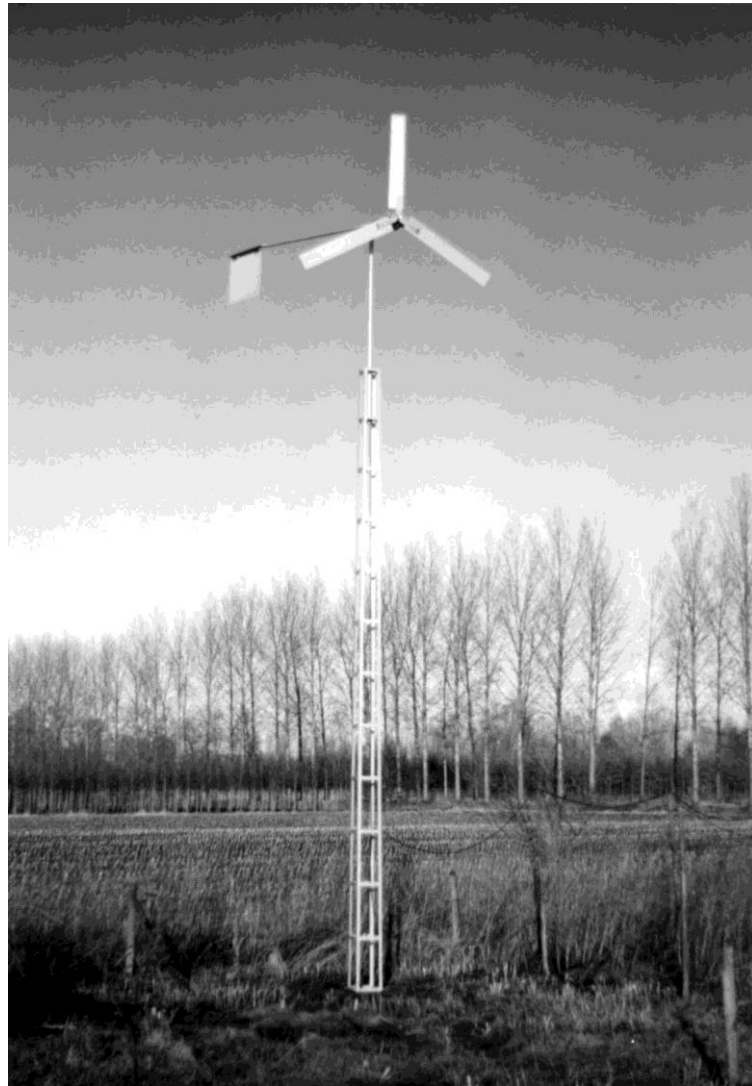


# **Rotor design and matching for horizontal axis wind turbines**



report KD 35

ing. Adriaan Kragten

## **Rotor design and matching for horizontal axis wind turbines**

Report number KD 35

Published by:  
Engineering office Kragten Design  
Populierenlaan 51  
5492 SG Sint-Oedenrode  
The Netherlands  
Telephone: +31 413 475770  
Website: [www.kdwindturbines.nl](http://www.kdwindturbines.nl)  
E-mail: [info@kdwindturbines.nl](mailto:info@kdwindturbines.nl)

1st print January 1999  
2nd print July 2004  
3rd digital version November 2015  
4nd digital version February 2017

It is allowed to copy this report for private use. The lay out is such that it can be printed at two sides of a sheet.

I thank Ir. P. T. Smulders for his comments on chapters 1 up to 5 of the manuscript. Paul Smulders was the head of the former Wind Energy Group of the Laboratory of Fluid Dynamics and Heat Transfer of the University of Technology Eindhoven and I worked with him for almost fifteen years. I also thank Dr. G. Stacey for his comments and for the English correction.

On the cover is the VIRYA-2.2 windmill which was developed by Kragten Design in 1998. The rotor geometry of this windmill is calculated using the design procedure given in chapter 5 of this report. Kragten Design supplies licences including manuals and building plans of a large range of VIRYA-windmills.

	<b>page</b>
<b>Contents</b>	3
<b>List of symbols</b>	4
<b>1 Introduction</b>	7
1.1 General	7
1.2 The wind turbine	8
<b>2 Energy and power of the wind</b>	9
<b>3 Lift and drag on aerofoils</b>	10
<b>4 Power extraction from the wind</b>	13
4.1 The rotor formulas	13
4.2 The Betz coefficient	14
4.3 Reasons why the maximum $C_p$ is lower than the Betz coefficient	17
4.3.1 Wake rotation	17
4.3.2 Finite number of blades	17
4.3.3 Profile drag	18
<b>5 Rotor Design</b>	24
5.1 General	24
5.2 Rotor parameters	24
5.3 Determination of the blade geometry	27
5.4 Examples of rotor design	31
5.4.1 Example no. 1	31
5.4.2 Example no. 2	34
5.5 Characteristics of the Gö 623 aerofoil	36
<b>6 Rotor characteristics</b>	40
6.1 General	40
6.2 Determination of $\lambda_{opt}$ , $C_{p\ max}$ and $\lambda_{unl}$	40
6.3 Determination of $C_{q\ start}$	42
6.4 Determination of the $C_p$ - $\lambda$ and $C_q$ - $\lambda$ curves	45
6.5 Example of rotor characteristics	47
<b>7 Rotors in yaw</b>	49
7.1 General	49
7.2 Determination of the yawing formulas	50
7.3 Example of yawing	51
<b>8 Matching of windmill rotor and generator</b>	53
8.1 General	53
8.2 Design parameters	53
8.3 Matching procedure	53
8.4 Example of matching	58
<b>9 References</b>	62

## List of symbols

A	area	(m <sup>2</sup> )
A <sub>k</sub>	area swept by a rotor blade with length k	(m <sup>2</sup> )
A <sub>r</sub>	rotor area	(m <sup>2</sup> )
A <sub>1</sub>	area of the stream-tube far before the rotor	(m <sup>2</sup> )
A <sub>2</sub>	area of the stream-tube far behind the rotor	(m <sup>2</sup> )
arctan	arc tangent	(-)
B	number of blades	(-)
b	width of a blade section, length of an aerofoil	(m)
c	blade chord	(m)
c <sub>lin</sub>	chord after linearisation	(m)
C <sub>m0.25</sub>	moment coefficient around the quarter chord point	(-)
c <sub>th</sub>	theoretical chord	(m)
C <sub>d</sub>	drag coefficient	(-)
C <sub>d</sub> /C <sub>l</sub> <sub>lin</sub>	C <sub>d</sub> /C <sub>l</sub> ratio after linearisation	(-)
C <sub>d</sub> /C <sub>l</sub> <sub>th</sub>	theoretical C <sub>d</sub> /C <sub>l</sub> ratio	(-)
C <sub>l</sub>	lift coefficient	(-)
C <sub>l</sub> <sub>lin</sub>	lift coefficient after linearisation	(-)
C <sub>l</sub> <sub>opt</sub>	optimum lift coefficient	(-)
C <sub>l</sub> <sub>th</sub>	theoretical lift coefficient	(-)
C <sub>p</sub>	power coefficient	(-)
C <sub>p</sub> <sub>max</sub>	maximum power coefficient	(-)
C <sub>p</sub> <sub>id</sub>	power coefficient for B = 4 and C <sub>d</sub> /C <sub>l</sub> = 0	(-)
C <sub>p</sub> <sub>th</sub>	theoretical power coefficient	(-)
C <sub>p</sub> <sub>δ</sub>	power coefficient at angle δ	(-)
C <sub>q</sub>	torque coefficient	(-)
C <sub>q</sub> <sub>δ</sub>	torque coefficient at angle δ	(-)
C <sub>q</sub> <sub>opt</sub>	optimum torque coefficient	(-)
C <sub>q</sub> <sub>start</sub>	starting torque coefficient	(-)
C <sub>t</sub>	thrust coefficient	(-)
C <sub>t</sub> <sub>δ</sub>	thrust coefficient at angle δ	(-)
D	rotor diameter	(m)
D	drag force	(N)
E	energy	(Ws)
E <sub>i</sub>	energy produced for a certain wind speed interval	(kWh)
E <sub>tot</sub>	total energy produced for all wind speed intervals	(kWh)
F <sub>t</sub>	thrust force acting on the rotor centre	(N)
F <sub>t</sub> <sub>δ</sub>	thrust force at angle δ	(N)
ΔF <sub>u</sub>	resulting force on a blade section in the direction of U	(N)
i	accelerating gear ratio	(-)
k	blade length	(m)
k'	effective blade length	(m)
L	lift force	(N)
M	aerodynamic moment	(Nm)
m	mass	(kg)

$n$	rotational speed of the rotor	(rpm)
$n_{\delta}$	rotational speed at angle $\delta$	(rpm)
$n_{\text{gen}}$	rotational speed of the generator	(rpm)
$P$	power	(W)
$P_{A1}$	power at area $A_1$	(W)
$P_{\delta}$	power at angle $\delta$	(W)
$P_{\text{el}}$	electrical generator power	(W)
$P_{\text{max}}$	maximum power	(W)
$\Delta P_u$	power generated by $\Delta F_u$	(W)
$P_{\delta}$	power at angle $\delta$	(W)
$P_{\text{mech}}$	mechanical generator power	(W)
$P_w$	power in the undisturbed wind	(W)
$Q$	torque	(Nm)
$Q_{\text{bl th}}$	theoretical torque of one blade	(Nm)
$Q_{\delta}$	torque at angle $\delta$	(Nm)
$Q_{\text{gen}}$	generator torque	(Nm)
$Q_{\text{rot th}}$	theoretical torque of the rotor	(Nm)
$Q_s$	sticking torque of the generator	(Nm)
$Q_{\text{start}}$	starting torque	(Nm)
$R$	radius at the blade tip	(m)
$Re$	Reynolds number	(-)
$Re_r$	local Reynolds number	(-)
$r$	local radius	(m)
$r_m$	radius at the middle of the blade	(m)
$\Delta T$	resulting thrust force on a blade section	(N)
$t$	time	(s)
$t$	profile thickness	(m)
$\tan$	tangent	(-)
$U$	local blade speed	(m/s)
$V$	undisturbed wind speed	(m/s)
$V_{\text{cut in}}$	wind speed at which the windmill starts to generate electricity	(m/s)
$V_{\text{rated}}$	wind speed at which the maximum electrical power is reached	(m/s)
$V_{\text{start}}$	wind speed at which the rotor starts rotating	(m/s)
$V_{\text{tip}}$	tip speed	(m/s)
$W$	relative wind speed	(m/s)

$\alpha$	angle of attack	(°)
$\alpha_{lin}$	angle $\alpha$ after linearisation	(°)
$\alpha_{th}$	theoretical angle $\alpha$	(°)
$\beta$	angle between the rotor plane and the zero-line of the aerofoil	(°)
$\beta_{lin}$	angle $\beta$ after linearisation	(°)
$\beta_{th}$	theoretical angle $\beta$	(°)
$\delta$	yaw angle, angle between wind direction and rotor axis	(°)
$\phi$	angle between direction of relative wind $W$ and rotor plane	(°)
$\phi_m$	mass flow	(kg/s)
$\gamma$	kinematic viscosity	(m <sup>2</sup> /s)
$\eta_{gen}$	generator efficiency factor (in KD reports it is given in %)	(-)
$\eta_{tr}$	transmission efficiency factor	(-)
$\rho$	air density	(kg/m <sup>3</sup> )
$\lambda$	tip speed ratio	(-)
$\lambda_d$	design tip speed ratio	(-)
$\lambda_r$	local speed ratio	(-)
$\lambda_{opt}$	optimum tip speed ratio	(-)
$\lambda_{r,d}$	local design speed ratio	(-)
$\lambda_{unl}$	unloaded tip speed ratio	(-)
$\lambda_\delta$	tip speed ratio at angle $\delta$	(-)
$\pi$	3.14159....	(-)
$\Omega$	angular velocity of the rotor	(rad/s)

## 1 Introduction

### 1.1 General

From 1975 until 1990 the Dutch organisation CWD (Consultancy services Wind energy Developing countries), published many reports about wind energy and water pumping windmills. I worked for almost fifteen year as a mechanical engineer and designer in the wind energy group of the University of Technology Eindhoven (TUE), one of the members of CWD.

Windmill rotors were designed at that time using reports which are now difficult to obtain. After CWD ceased to function in July 1990, I started my own private engineering office Kragten Design (KD), specialising in the development of small electricity generating windmills and in providing a wind energy consultancy service. I wrote many reports on generator tests and also a report on matching windmill rotor and generator.

I decided to write and publish this report KD 35, because I believe there is a need for such a report in which the basic knowledge of rotor design and matching is brought together, so that only one report is necessary to design a windmill rotor. The most important reports which I used are:

- 1 Horizontal axis fast running wind turbines for developing countries, CWD publication 76-1 (ref. 9.1).
- 2 Rotor Design for horizontal axis windmills, CWD publication 77-1 (ref. 9.2).
- 3 Catalogue of Aerodynamic Characteristics of Aerofoils in the Reynolds number range  $10^4$ - $10^6$ , TUE report R 443 D, (ref. 9.3).
- 4 The Gö 622, Gö 623, Gö 624 and Gö 625 airfoils with thickness/chord ratios of respectively 8 %, 12 %, 16 % and 20 % for use in windmill rotor blades, report KD 463 (ref. 9.4).
- 5 Rotor Design part 2, TUE report R 1078 D, (ref. 9.5).
- 6 Rotors, TUE report (has no R number), (ref. 9.6).
- 7 Matching of windmill rotor and generator (in Dutch), report KD 05, (ref. 9.7).

The report Rotors (ref. 9.6) and Rotor Design part 2 (ref. 9.5) link together and replace the original CWD publication Rotor Design for horizontal axis windmills (ref. 9.2).

Although knowledge from existing reports is used, no parts were simply copied. The whole report was typed anew (in Word 97 and Windows 95). All figures were also redrawn (the ordinary figures using the drawing option of Word 97 and the graphs in Excel 97). Chapters 1 to 4 are rewritten completely. Chapters 5, 6 and 7 are roughly based on Rotor Design part 2 (ref. 9.5), but the contents and the examples have been changed considerably. Chapter 8 is more or less a translation of KD report KD 05 (ref. 9.7).

Chapters 2, 3 and 4 give general aerodynamic knowledge on horizontal axis wind turbines. Chapter 5 gives the rotor design theory. Chapter 6 provides a simple theory to estimate rotor characteristics. Chapter 7 discusses the influence of yawing of the rotor on the rotor formulas. This knowledge is important if the windmill has a safety system which turns the rotor out of the wind. Chapter 8 provides information on matching rotor and generator. Chapters 5, 6, 7 and 8 conclude with an example in which the theory is demonstrated.

On request, I am available to give courses on wind energy based on the knowledge in this report. The course can be given in English or in Dutch. Questions and answers are available to check the knowledge of each chapter (report KD 196, ref. 9.11).

## 1.2 The wind turbine

In this publication horizontal axis wind turbines for electricity generation are discussed. The rotor of the wind turbine is generally coupled to the generator by a transmission system (see fig. 1.1).

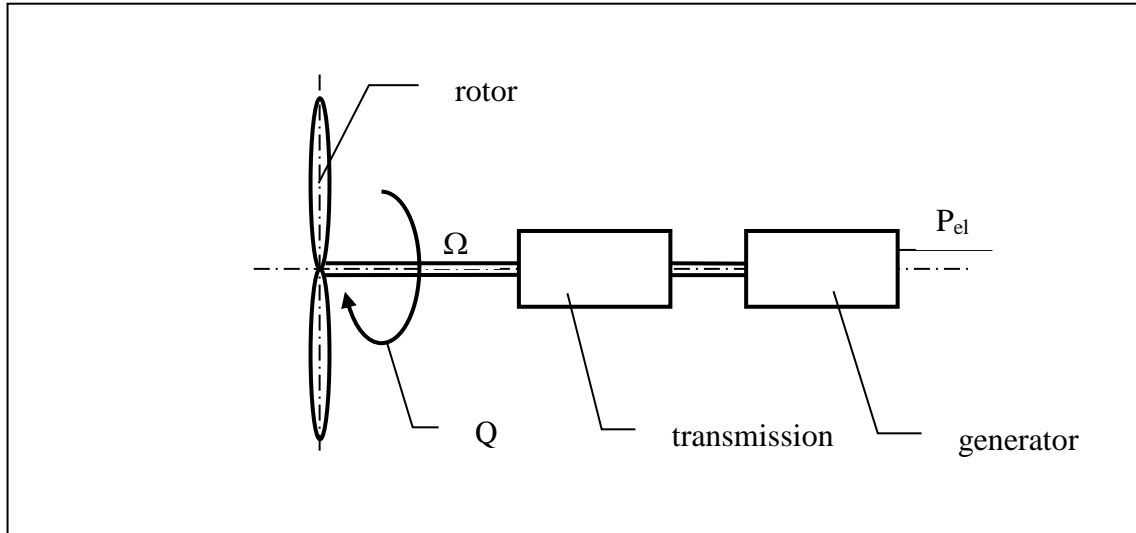


Fig. 1.1 The wind turbine

The rotor generates a torque  $Q$  on the rotor shaft with an angular velocity  $\Omega$ . The power transmitted by the rotor shaft is given by:

$$P = Q * \Omega \quad (\text{W}) \quad (1.1)$$

The electrical generator power  $P_{el}$  is less than the rotor power because of the efficiency of the transmission  $\eta_{tr}$  and the efficiency of the generator  $\eta_{gen}$ . So  $P_{el}$  is given by:

$$P_{el} = \eta_{tr} * \eta_{gen} * P \quad (\text{W}) \quad (1.2)$$

A very important parameter for the windmill characteristic is the tip speed ratio  $\lambda$ , being the ratio between the tip speed  $V_{tip}$  and the undisturbed wind speed  $V$ . So  $\lambda$  is given by:

$$\lambda = V_{tip} / V \quad (-) \quad (1.3)$$

The tip speed  $V_{tip}$  for a rotor with radius  $R$  is given by:

$$V_{tip} = \Omega * R \quad (\text{m/s}) \quad (1.4)$$

Combining formula 1.4 and 1.3 we get:

$$\lambda = \Omega * R / V \quad (-) \quad (1.5)$$

More specific formulas for  $P$  and  $Q$  are given in chapter 4.



## 2 Energy and power of the wind

The kinetic energy of a moving body with mass  $m$  and speed  $V$  is given by:

$$E = \frac{1}{2} m V^2 \quad (\text{Ws}) \quad (2.1)$$

With air flow, it is conventional to consider the energy of a mass flow per second  $\phi_m$  passing through a certain area  $A$  (see fig. 2.1).

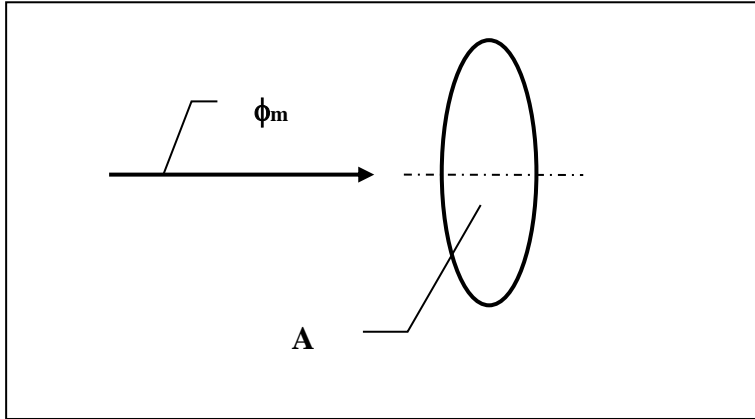


Fig. 2.1 Mass flow through area A

With  $\phi_m = m / t$  formula 2.1 can be rewritten as:

$$E = \frac{1}{2} \phi_m * t * V^2 \quad (\text{Ws}) \quad (2.2)$$

The mass flow per second through area  $A$  is given by:

$$\phi_m = V * A * \rho \quad (\text{kg/s}) \quad (2.3)$$

The density  $\rho$  of air is about  $1.2 \text{ kg/m}^3$  at a temperature of  $20^\circ$  Celsius at sea level.

Combining formula 2.3 and 2.2 we get:

$$E = \frac{1}{2} \rho V^3 * A * t \quad (\text{Ws}) \quad (2.4)$$

Power is the energy per second and is found by dividing  $E$  by the time  $t$ .

So the power  $P_w$  of the undisturbed wind is given by:

$$P_w = \frac{1}{2} \rho V^3 * A \quad (\text{W}) \quad (2.5)$$

If we take as an example for  $A$ , a circle with a radius  $R = 1 \text{ m}$ , and if the wind speed is  $V = 5 \text{ m/s}$  it can be calculated that  $P_w = 235.6 \text{ W}$ . Not all this power can be extracted from the wind by a wind turbine. In chapter 4.2 and 4.3 this will be explained in more detail.

### 3 Lift and drag on aerofoils

A horizontal axis wind turbine extracts energy from the wind by making use of the lift force acting on the rotor blade. A rotor blade is usually shaped like an aerodynamic aerofoil and therefore some general information about aerofoils is relevant.

First we consider an aerofoil which is not rotating but more like an aerofoil as it is tested in a wind tunnel or in flight. The air flow over the aerofoil causes a large negative pressure on the convex upper side of the aerofoil and a positive pressure on the flat lower side of the aerofoil. This pressure difference causes two different resulting forces being the lift  $L$  and the drag  $D$ . The lift is defined as the force perpendicular to the direction of the wind  $W$  and the drag is the force in the direction of the wind. There is also a moment  $M$  which is normally centred around a point which lies  $\frac{1}{4}$  of the chord back from the leading edge (see fig. 3.1).

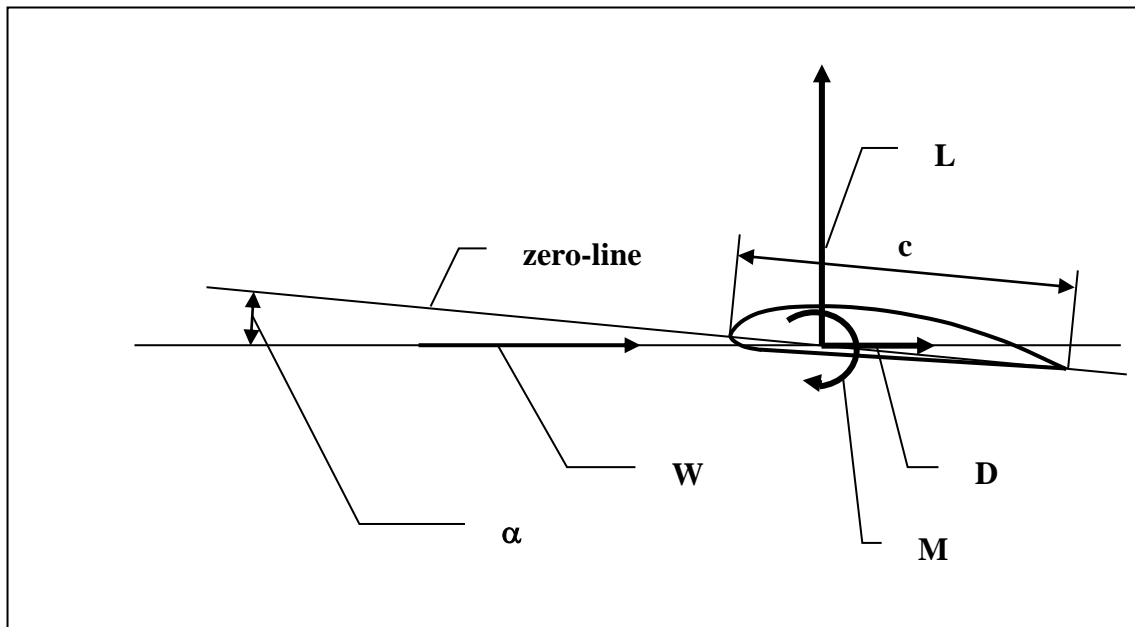


Fig. 3.1 Lift, drag and moment acting on an aerofoil

The position of the aerofoil is defined by the angle of attack  $\alpha$  which is the angle between the direction of the wind  $W$  and the zero-line of the aerofoil. The zero-line is generally defined as the line through the leading edge and the trailing edge but for some aerofoils the flat lower side is taken as zero-line.

An aerofoil has a certain chord  $c$  and a certain length  $b$ . The thickness for a certain chord in combination with the shape determines the type of aerofoil. The ratio  $b / c$  is labelled the aspect ratio. If an aerofoil is tested in a wind tunnel generally it has a length identical to the width of the measuring section of the wind tunnel. The aspect ratio for this situation is effectively infinite because the wind tunnel walls prevent tip effects.

Lift and drag can be measured for a constant wind speed as a function of the angle of attack  $\alpha$ . The lift coefficient  $C_l$  and the drag coefficient  $C_d$  are given by:

$$C_l = \frac{L}{\frac{1}{2} \rho W^2 * c * b} \quad (-) \quad (3.1)$$

$$C_d = \frac{D}{\frac{1}{2} \rho W^2 * c * b} \quad (-) \quad (3.2)$$

The moment coefficient  $C_{m0.25}$  around the quarter chord point is given by:

$$C_{m0.25} = \frac{M}{\frac{1}{2} \rho W^2 * c^2 * b} \quad (-) \quad (3.3)$$

Generally the direction of the moment is taken as clockwise (nose-up). The moment coefficient itself is negative and near constant for small angles  $\alpha$ . So the moment has a tendency to decrease the angle of attack.

In aerofoil books such as (ref. 9.3), the coefficients  $C_l$ ,  $C_d$  and  $C_{m0.25}$  are given in graphs as a function of  $\alpha$ . Sometimes  $C_l$  is provided as a function of  $C_d$ . Sometimes the results are given in tables. For the rotor design procedure described in chapter 5, one needs only a  $C_l$ - $\alpha$  curve and a  $C_l$ - $C_d$  curve. These curves are given for the Gö 623 aerofoil in section 5.5.

The aerodynamic characteristics depend on the Reynolds number  $Re$  which is given by:

$$Re = W * c / \gamma \quad (-) \quad (3.4)$$

$\gamma$  is the kinematic viscosity of air which is about  $15 * 10^{-6}$  (m<sup>2</sup>/s). Normally aerodynamic characteristics, for a certain aerofoil, are given for a range of Reynolds numbers. Small windmills operate at rather low Reynolds numbers. Most aerofoils have been measured at rather high Reynolds numbers because they are used for aeroplane wings which have large chords and fly at high speeds.

If an aerofoil is rotating, as in the case for a windmill blade, the situation is different from an aerofoil tested in a wind tunnel. The situation is given in fig. 3.2 for a small blade section with length  $\Delta r$  taken near the blade tip.

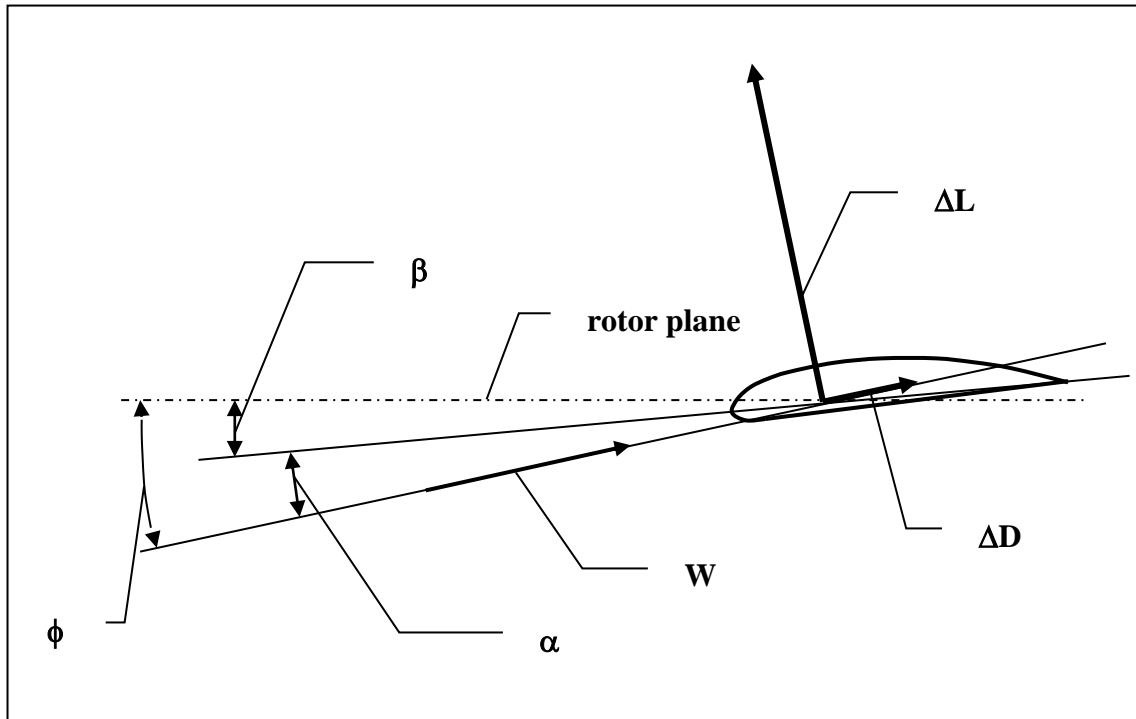


Fig. 3.2 Lift and drag forces  $\Delta L$  and  $\Delta D$  acting on a rotating blade section

The local blade speed  $U$  near the blade tip is much larger than the absolute wind speed at the rotor plane (see fig. 4.4). The relative wind  $W$  therefore makes a large angle with the direction of the absolute wind speed and a small angle with the rotor plane which is the plane perpendicular to the rotor shaft in which the blades rotate. The angle between the relative wind  $W$  and the rotor plane is labelled  $\phi$ . The angle between the zero-line of the aerofoil and the rotor plane is the blade setting angle  $\beta$ . The angle  $\alpha$  is equivalent to the angle  $\alpha$  used in the wind tunnel tests. It can be seen that  $\beta = \phi - \alpha$ .

## 4 Power extraction from the wind

### 4.1 The rotor formulas

Formula 2.5 gives the power available in the undisturbed wind. The power extracted from the wind by a wind turbine is given by:

$$P = C_p * \frac{1}{2} \rho V^3 * \pi R^2 \quad (\text{W}) \quad (4.1)$$

$\pi R^2$  is the rotor area  $A_r$  swept by the rotor blades. The maximum  $C_p$  value for a well designed rotor lies between 0.4 and 0.45.

Combining formula 4.1 and 1.2:  $P_{el} = \eta_{tr} * \eta_{gen} * P$ , we get:

$$P_{el} = C_p * \eta_{tr} * \eta_{gen} * \frac{1}{2} \rho V^3 * \pi R^2 \quad (\text{W}) \quad (4.2)$$

The torque  $Q$  is given by:

$$Q = C_q * \frac{1}{2} \rho V^2 * \pi R^3 \quad (\text{Nm}) \quad (4.3)$$

The tip speed ratio  $\lambda$  is given by formula 1.5 as  $\lambda = \Omega * R / V$ . Formula 1.1 can be written as  $\Omega = P / Q$ .

Combining formula 1.5 and 1.1 we get:

$$\lambda = \frac{P * R}{Q * V} \quad (-) \quad (4.4)$$

Combining formula 4.4, 4.3 and 4.1 we get:

$$\lambda = C_p / C_q \quad (-) \quad (4.5)$$

The optimum tip speed ratio of a rotor  $\lambda_{opt}$  is the tip speed ratio where the power coefficient  $C_p$  has a maximum. The corresponding value for  $C_q$  is labelled  $C_{q\ opt}$ . The best way to determine  $\lambda_{opt}$  is to measure a scale model of the rotor in the wind tunnel at the correct Reynolds number. The design tip speed ratio of a rotor  $\lambda_d$  is the tip speed ratio for which the rotor is designed. If the correct design procedure is used, and if the rotor is made accurately,  $\lambda_{opt}$  and  $\lambda_d$  will be about the same. In most literature  $\lambda$  is used for  $\lambda_{opt}$  and  $\lambda_d$ . The actual tip speed ratio  $\lambda$  of a rotor at a certain wind speed depends on the load. More information about  $C_p$ - $\lambda$  curves is given in chapter 6.  $\lambda_{opt}$  is a function of rotor design. Slow running multi-bladed rotors used for water pumping windmills have  $\lambda_{opt}$  between 1 and 2. Old fashioned Dutch windmills used for grain milling have four bladed rotors with  $\lambda_{opt}$  of about 2.5. Fast running wind turbines used for the generation of electricity have two or three bladed rotors with  $\lambda_{opt}$  between 4 and 10.

For  $\lambda = \lambda_{opt}$ ,  $C_p = C_{p\ max}$  and  $C_q = C_{q\ opt}$ , formula 4.5 changes into:

$$\lambda_{opt} = C_{p\ max} / C_{q\ opt} \quad (-) \quad (4.6)$$

The angular velocity  $\Omega$  is given by:

$$\Omega = \pi * n / 30 \quad (\text{rad/s}) \quad (n \text{ is the rotational speed in rpm}) \quad (4.7)$$

Combining formula 4.7 and 1.5 we get:

$$n = 30 * \lambda * V / \pi R \quad (\text{rpm}) \quad (4.8)$$

## 4.2 The Betz coefficient

Not all the kinetic energy can be extracted from the wind because this would result in the reduction of the wind speed to zero and this implies that no air is flowing through the rotor area. It was Betz who developed a theory in 1926 which gives the absolute maximum value for  $C_p$ .

The pressure just before the windmill rotor is somewhat higher than the pressure just behind the rotor if the rotor extracts energy from of the wind. This pressure difference forms a resistance to the air flowing through the rotor. Therefore the wind has a tendency to flow around the rotor instead of through it.

The air particles flowing through the rotor form a stream-tube. This stream-tube is bounded by air particles which just touch the blade tip. The distance between the stream line of these particles and the rotor axis increases as a particle is followed from a position far upstream from the rotor up to a position far downstream. This means that the stream-tube is expanding. The shape of the stream-tube is illustrated in fig. 4.1. Theoretically far upstream and far downstream the rotor means at an infinite distance from the rotor but in practice a distance of about three rotor diameters is enough to describe the principle.

The cross sectional area of the stream-tube far in front of the rotor is labelled  $A_1$ . The swept area of the rotor is labelled  $A_r$ . The cross sectional area of the stream-tube far behind the rotor is labelled  $A_2$ . At  $A_1$  the wind speed is undisturbed. This undisturbed wind speed is labelled  $V$ . Betz showed that maximum power is extracted from the wind if the wind speed at  $A_r$  is  $2/3 V$  and if the wind speed at  $A_2$  is  $1/3 V$ . If the air is considered incompressible, the product of the wind speed and the area must be constant so:

$$A_1 * V = A_r * 2/3 V = A_2 * 1/3 V. \quad (4.9)$$

This results in  $A_1 = 2/3 A_r$  and  $A_2 = 2 A_r$ .

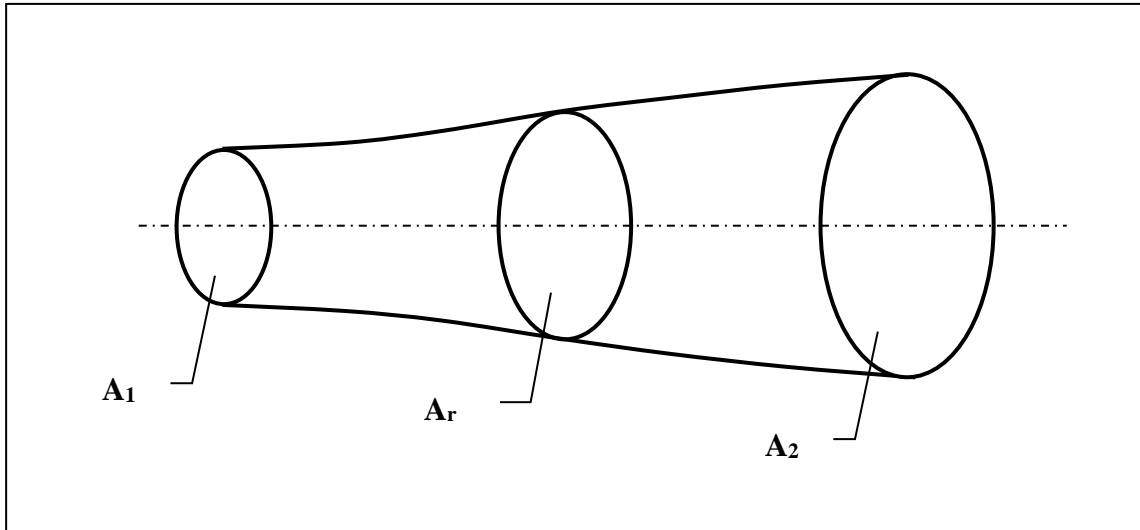


Fig. 4.1 Stream-tube of the air flowing through a windmill rotor

Betz used momentum theory and considered the windmill rotor as a so-called actuator disk. This is simply a mechanism which extracts energy from the wind. It needs not necessarily to be a rotating windmill rotor with blades.

The maximum power  $P_{\max}$ , which the rotor can extract from the wind if all losses are neglected, is the power at  $A_1$  minus the power at  $A_2$ .

Combining formula 2.5:  $P_w = \frac{1}{2}\rho V^3 * A$  and  $A_1 = \frac{2}{3} A_r$  and  $A_2 = 2 A_r$  we get:

$$P_{\max} = \frac{1}{2}\rho V^3 * \frac{2}{3} A_r - \frac{1}{2}\rho (1/3V)^3 * 2 A_r \text{ or}$$

$$P_{\max} = 16/27 * \frac{1}{2}\rho V^3 * A_r \quad (\text{W}) \quad (4.10)$$

The power available in the undisturbed wind at  $A_r$  is given by formula 2.5 as:

$$P_w = \frac{1}{2}\rho V^3 * A_r.$$

The ratio between the maximum power which can be extracted from the wind at  $A_r$  and the power in the undisturbed wind at  $A_r$  (no rotor in place), is called the Betz coefficient. Combining formula 4.10 and 2.5 we get:

$$\text{Betz coefficient} = P_{\max} / P_w = 16/27 = 0.59 \quad (-) \quad (4.11)$$

The Betz coefficient is not equal to the aerodynamic efficiency of the energy transformation. For the aerodynamic efficiency, the whole stream-tube has to be taken into account. So the generated power should not be compared to the power flowing through the plane  $A_r$  but to the power flowing through the plane  $A_1$ . As  $A_1$  is  $\frac{2}{3}$  of  $A_r$ , the maximum aerodynamic efficiency is a factor  $\frac{3}{2}$  larger than the maximum  $C_p$  and so it is  $\frac{3}{2} * \frac{16}{27} = \frac{8}{9}$ .

The pressure difference over the rotor area results in a resulting thrust force  $F_t$  acting on the centre of the rotor.  $F_t$  is given by:

$$F_t = C_t * \frac{1}{2} \rho V^2 * \pi R^2 \quad (\text{N}) \quad (4.12)$$

Betz found that  $C_t = 8/9$  if the wind speed at the rotor plane is reduced to  $2/3 V$ . For a real windmill  $C_t$  generally is somewhat lower than the Betz value. For the rotor of the VIRYA-3.3 windmill, which is used in the examples,  $C_t$  is about 0.7 for  $\lambda = \lambda_{opt}$ . If the rotor is running unloaded, so for  $\lambda = \lambda_{unl}$ ,  $C_t$  is about the same.  $C_t$  is much lower if the rotor is not running, that is  $\lambda = 0$ . For this condition  $C_t$  is determined by the combined drag on all the blades.  $C_t$  for  $\lambda = 0$  is much lower for rotors with a high  $\lambda_{opt}$  than for rotors with a low  $\lambda_{opt}$  because rotors with a high  $\lambda_{opt}$  have a much lower total blade area (see chapter 5).



### 4.3 Reasons why the maximum $C_p$ is lower than the Betz coefficient

The maximum power coefficient  $C_{p \max}$  of a real windmill rotor is smaller than the Betz coefficient because of four effects: wake rotation, finite number of blades, profile drag and an effective blade length  $k$  which is shorter than  $R$ . The last effect is given by formula 6.3.

#### 4.3.1 Wake rotation

The power  $P$  of a windmill rotor is given by formula 1.1:  $P = Q * \Omega$ .

Two rotors with the same diameter but with different  $\lambda_{opt}$  can generate about the same power at the same wind speed. However the torque of the rotor with the lowest  $\lambda_{opt}$  must be higher since  $\Omega$  is lower. As the wind exerts a torque on the rotor, the rotor will exert a torque on the wind in the opposite direction. This torque results in rotation of the wake in and behind the rotor. This wake rotation absorbs some power resulting in a decrease in  $C_p$ . This decrease in  $C_p$ , which was described by Glauert in 1935, is greater for low  $\lambda_{opt}$ . This effect is shown in fig. 4.2. This figure is made from table 1.1 of (ref. 9.1). The ideal  $C_p$  value for  $B = \infty$  and  $C_d/C_l = 0$  is labelled  $C_{p \text{ id}}$ .

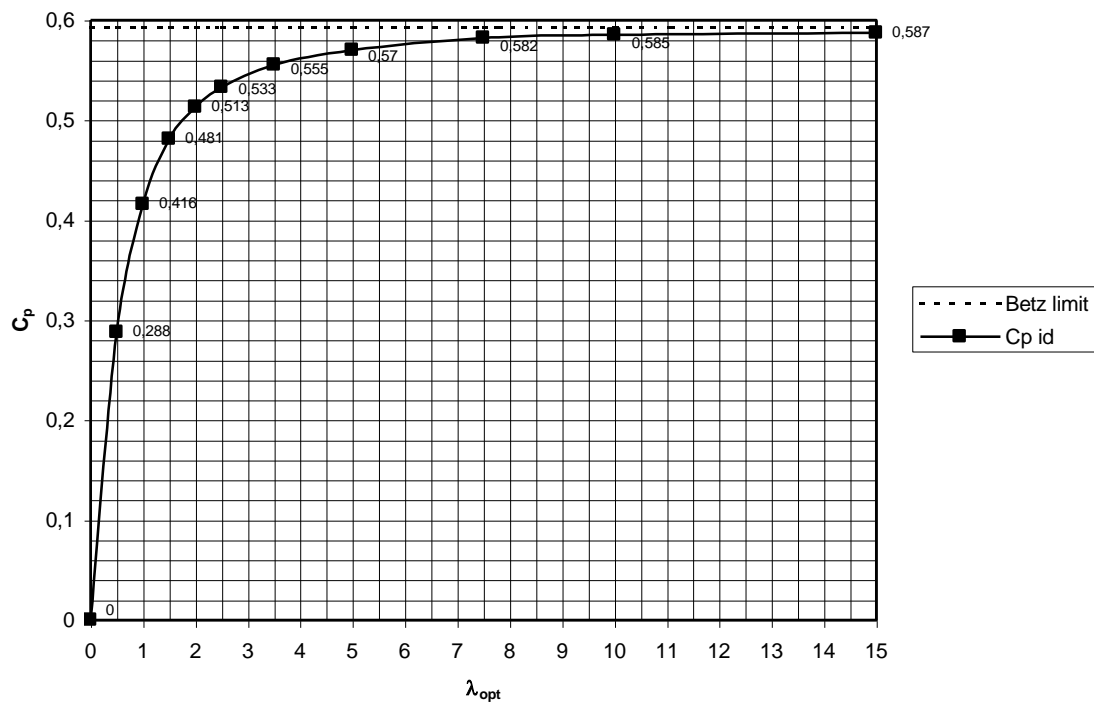


Fig. 4.2 Effect of wake rotation on  $C_p$  as a function of  $\lambda_{opt}$  for  $B = \infty$  and  $C_d/C_l = 0$

#### 4.3.2 Finite number of blades

In the Betz theory an actuator disk replaces the rotor. A real rotor has a finite number of blades and each blade has an aerodynamic shape (see fig. 3.2). The air flow over the aerofoil causes a large negative pressure on the convex upper side and a positive pressure on the flat lower side. This pressure difference cannot be maintained at the blade tip because air will flow from the lower side to the upper side. This causes tip losses which are more important with less rotor blades. The influence of the number of blades on  $C_p$  as a function of  $\lambda_{opt}$  for  $C_d/C_l = 0$  is given in fig. 4.3.

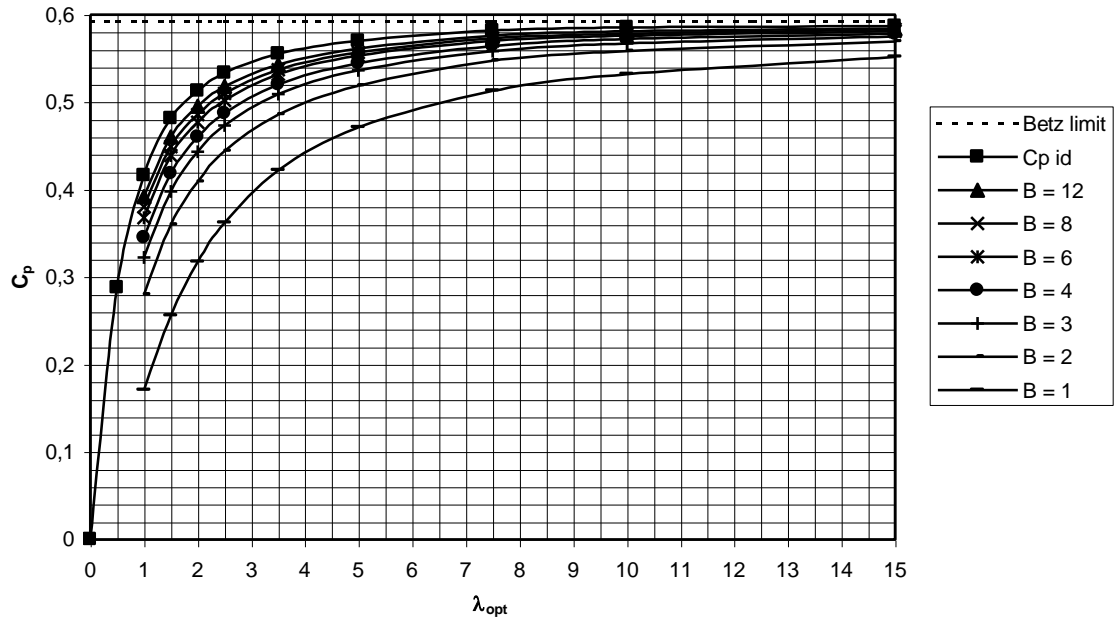


Fig. 4.3  $C_p$  as a function of the number of blades  $B$  and  $\lambda_{opt}$  for  $C_d/C_l = 0$

### 4.3.3 Profile drag

In fig. 3.2 the position of the blade aerofoil was given as near the blade tip. The direction of  $U$ ,  $W$  and the absolute wind speed is illustrated in the speed diagram in fig. 4.4. The wake rotation is neglected and the absolute wind speed  $2/3 V$  therefore can be drawn perpendicular to the rotor plane.

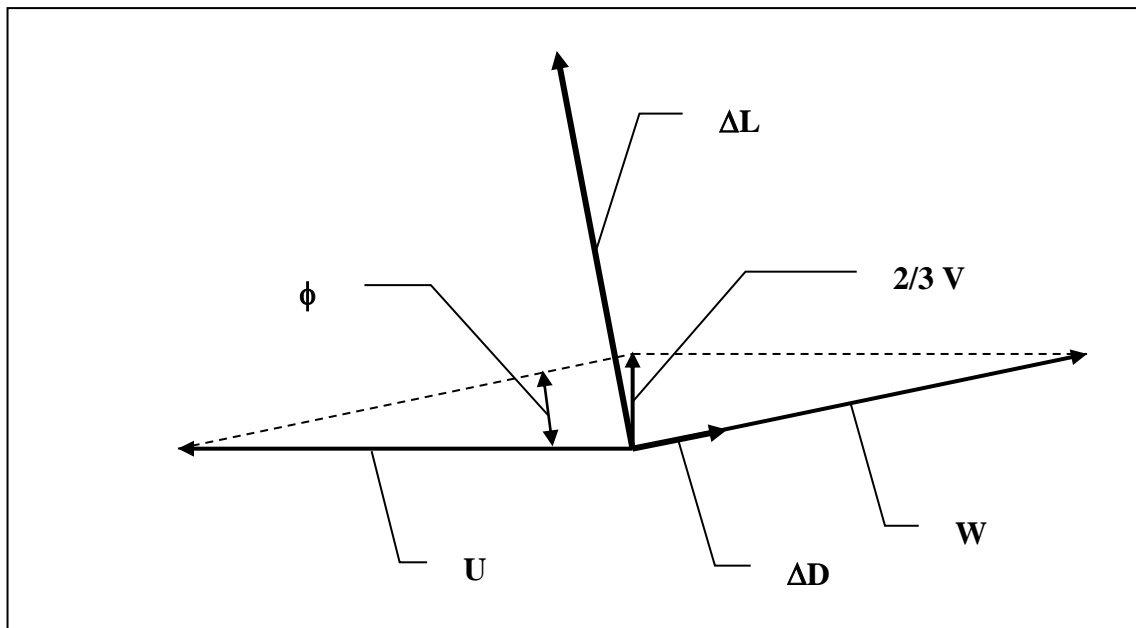


Fig. 4.4 Speed diagram for a section of a rotating rotor blade near the blade tip

The lift force  $\Delta L$  and the drag force  $\Delta D$  for the blade section with length  $\Delta r$  have also been shown in fig. 4.4. Both forces can be resolved into components in the rotor plane and components perpendicular to the rotor plane. The resulting force  $\Delta F_u$ , acting on the chosen section in the direction of  $U$ , is given by:

$$\Delta F_u = \Delta L \sin\phi - \Delta D \cos\phi \quad (\text{N}) \quad (4.13)$$

The product  $\Delta F_u * U$  is the Power  $\Delta P_u$  produced by the blade section. The sum of  $\Delta P_u$  of all blade sections of all blades is the total power  $P$  of the rotor as given by formula 4.1. Formula 4.13 shows that drag has a negative influence on the power and therefore on  $C_p$ . The effect of the drag is often represented by the  $C_d/C_l$  ratio instead of by the difference between the lift and drag components.

The thrust force  $\Delta T$ , acting on the chosen section perpendicular to the rotor plane, is given by:

$$\Delta T = \Delta L \cos\phi + \Delta D \sin\phi \quad (\text{N}) \quad (4.14)$$

So both lift and drag contribute to the thrust. The sum of  $\Delta T$  for all blade sections of all the blades is the total thrust  $F_t$  as given in formula 4.12.

The influence of the  $C_d/C_l$  value on  $C_p$  as a function of  $\lambda_{opt}$  is given in figures 4.5 to 4.11 for number of blades  $B$  between 1 and 12. This value of  $C_p$  is labelled  $C_{p\ th}$  because it is only achieved if the blade has an aerofoil from the blade tip right to the hub centre and if the  $C_d/C_l$  value is achieved along the whole blade. In reality the aerofoil begins only at a certain distance from the hub centre and this causes a reduction in  $C_{p\ th}$ . The reduced value is labelled  $C_{p\ max}$  (see section 6.2).

Figures 4.5 to 4.11 are taken from (ref. 9.2). The theory to derive these figures is given in (ref. 9.1). The required formulas to derive these seven figures, and fig. 4.3, are:

$$C_p = (C_{p\ id} - 16/27 * C_d/C_l * \lambda_{opt}) (1 - 1.386/B * \sin^{1/2}\phi)^2 \quad (-) \quad (4.15)$$

$$\phi = 2/3 \arctan 1 / \lambda_{opt} \quad (^\circ) \quad (4.16)$$

The  $C_{p\ th} - \lambda$  curves presented in fig. 4.5 to 4.11 are not  $C_p - \lambda$  curves (see chapter 6) for a specific windmill rotor. They show the maximum  $C_p$  which can be realised for a certain combination of  $B$ ,  $\lambda_{opt}$  and  $C_d/C_l$ . The  $C_p - \lambda$  curve of the rotor touches the  $C_{p\ th} - \lambda$  curve for a certain  $C_d/C_l$  value close to the top of the  $C_p - \lambda$  curve.

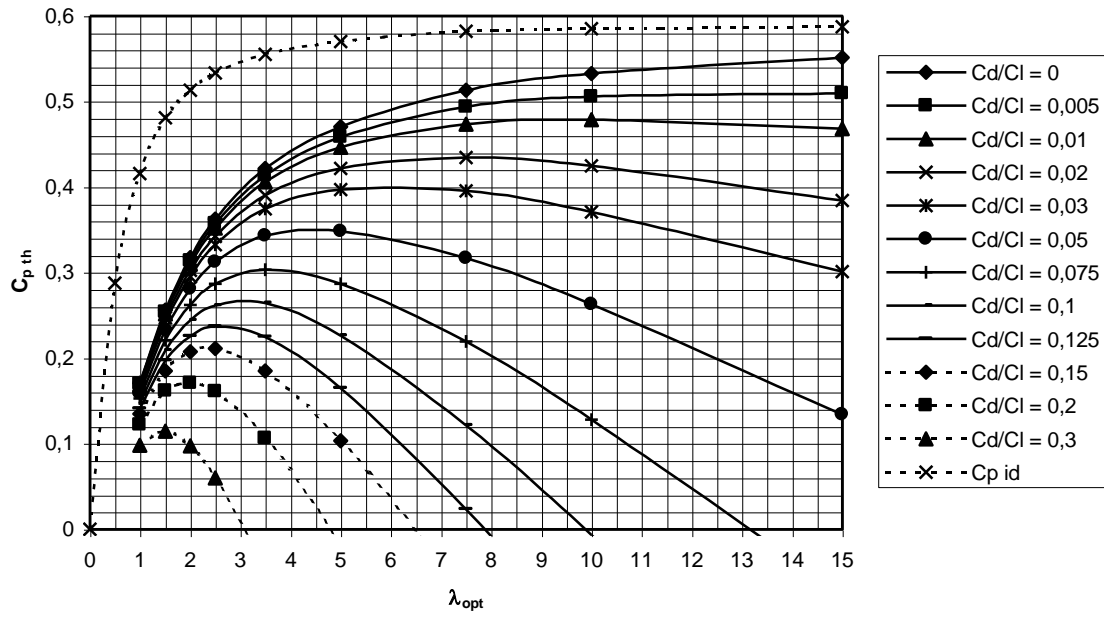


Fig. 4.5  $C_{p th}$  as a function of  $\lambda_{opt}$  and the  $C_d/C_l$  value for a 1-bladed rotor

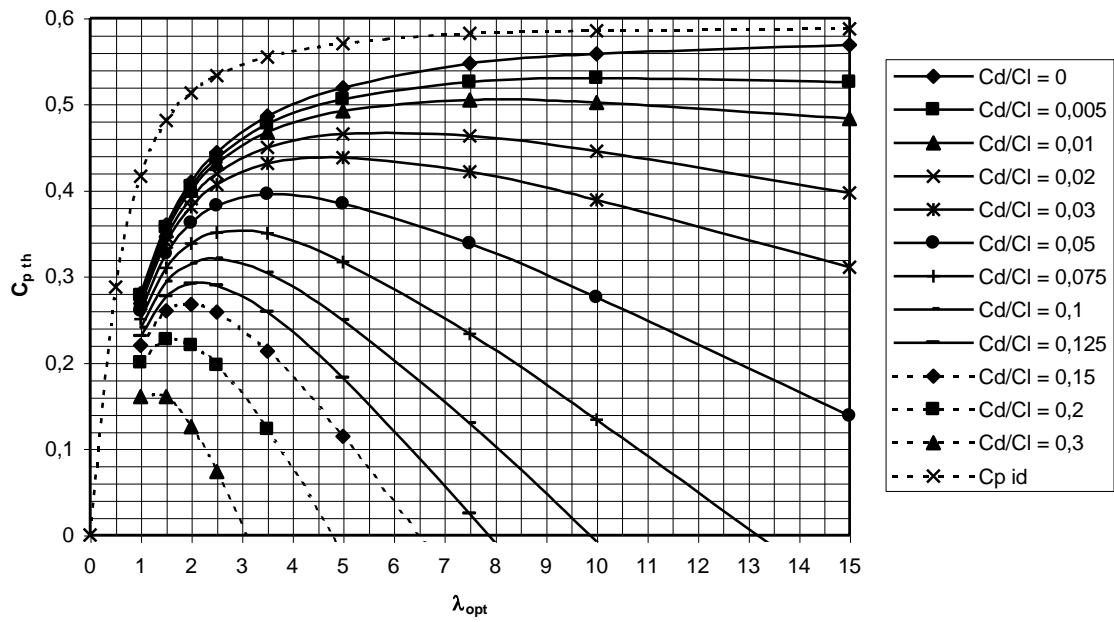


Fig. 4.6  $C_{p th}$  as a function of  $\lambda_{opt}$  and the  $C_d/C_l$  value for a 2-bladed rotor

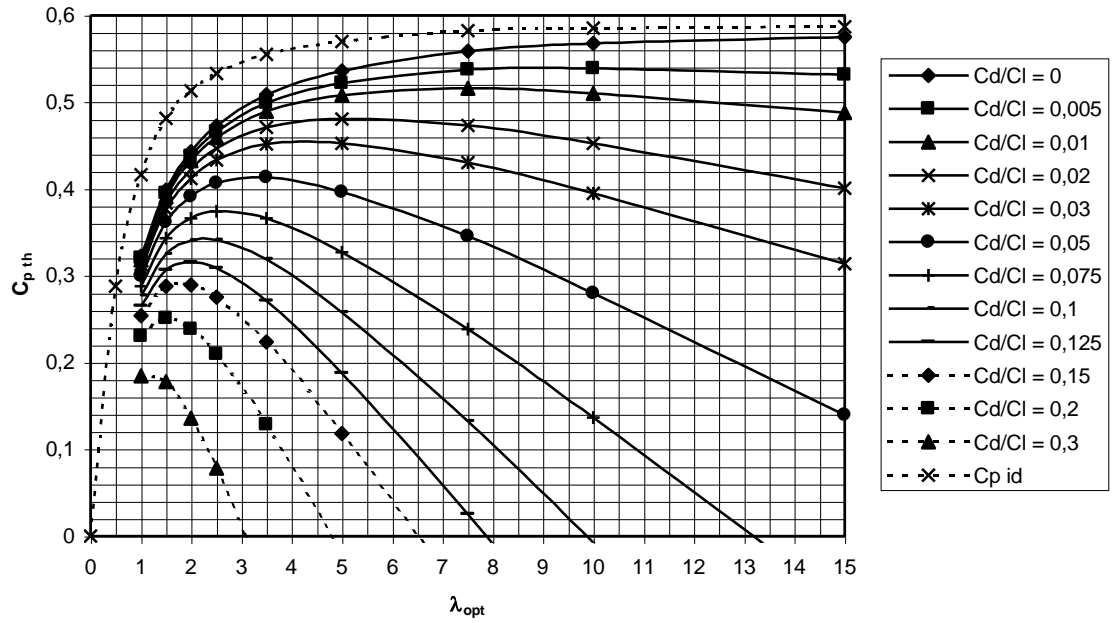


Fig. 4.7  $C_{p\ th}$  as a function of  $\lambda_{opt}$  and the  $C_d/C_l$  value for a 3-bladed rotor

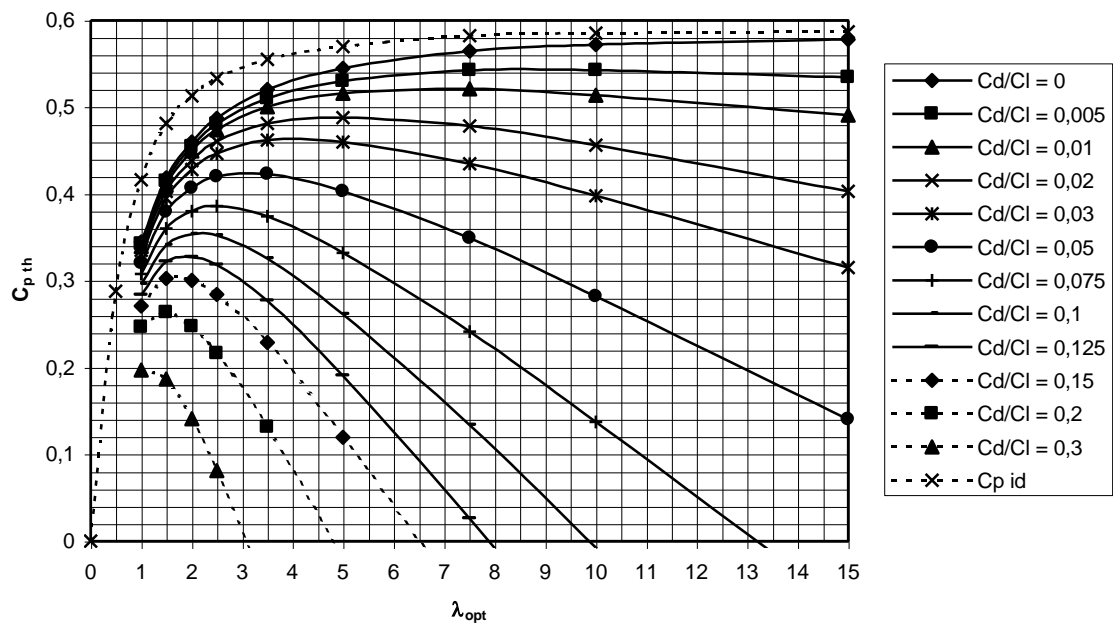


Fig. 4.8  $C_{p\ th}$  as a function of  $\lambda_{opt}$  and the  $C_d/C_l$  value for a 4-bladed rotor

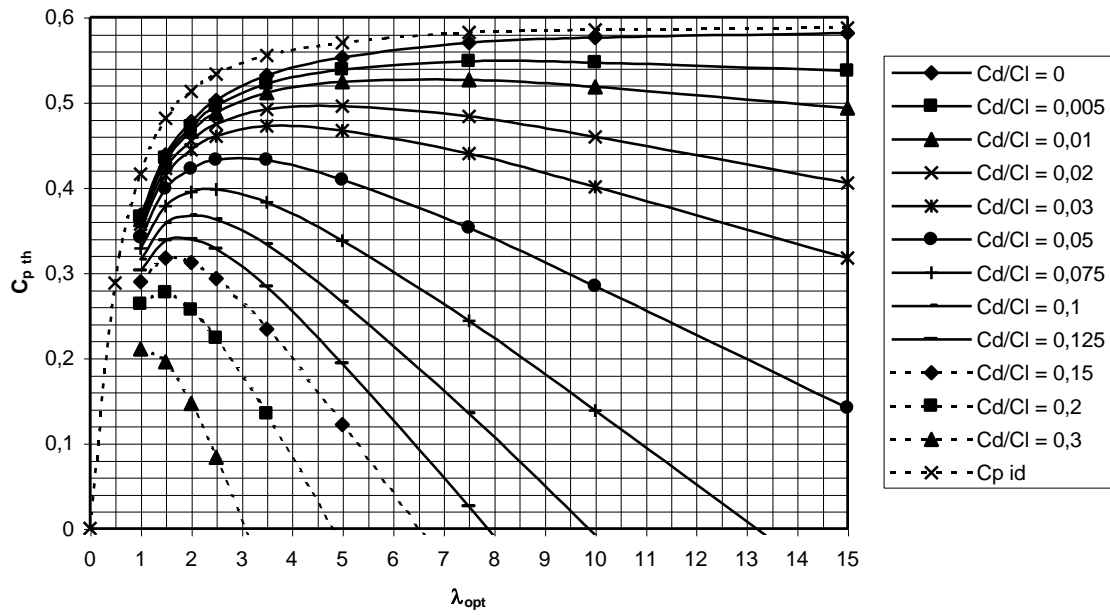


Fig. 4.9  $C_{p,th}$  as a function of  $\lambda_{opt}$  and the  $C_d/C_l$  value for a 6-bladed rotor

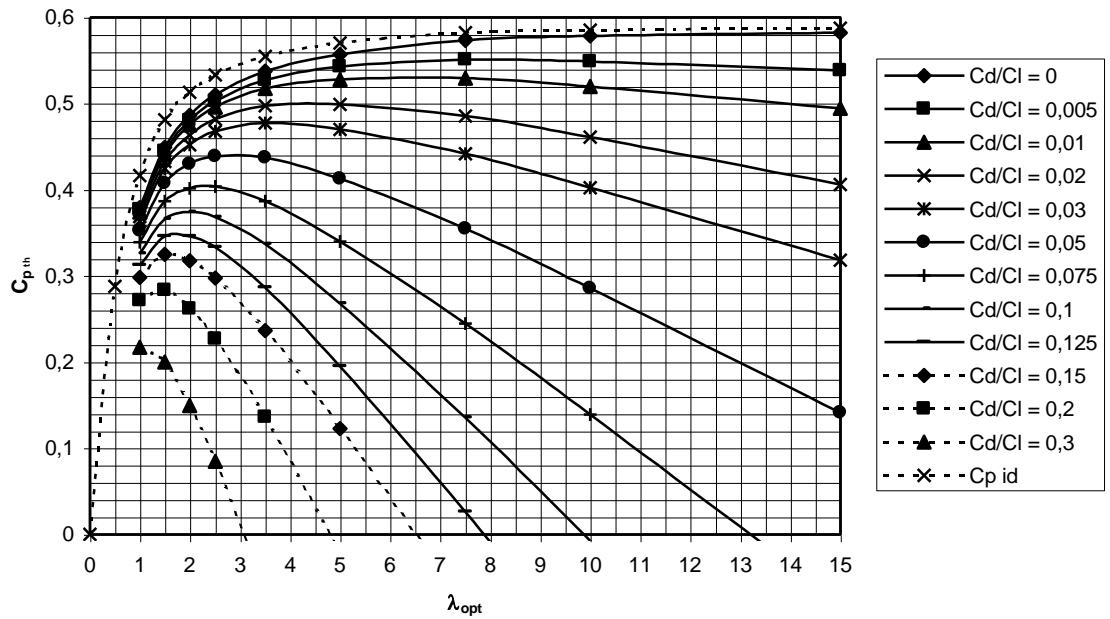


Fig. 4.10  $C_{p,th}$  as a function of  $\lambda_{opt}$  and the  $C_d/C_l$  value for a 8-bladed rotor

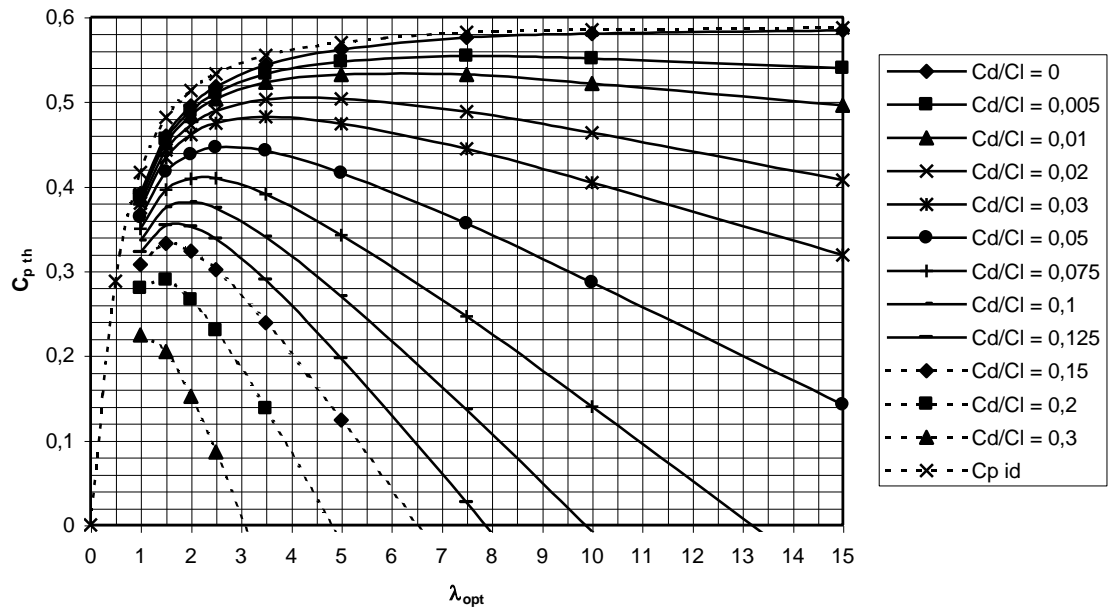


Fig. 4.11  $C_{p\ th}$  as a function of  $\lambda_{opt}$  and the  $C_d/C_l$  value for a 12-bladed rotor

## 5 Rotor design

### 5.1 General

This chapter is based on chapter 5 of Rotor Design part 2 (ref. 9.5). All rotors of the former CWD windmills, all rotors of the VIRYA windmills of Kragten Design and many other rotors have been designed according to the formulas given in this chapter. Wind tunnel measurements on many scale model rotors of the CWD windmills have demonstrated that rotors are obtained with good performance.

The original theory was derived by Glauert in 1935. He combined the momentum theory with the blade element theory which describes the forces on the individual blades. It is beyond the scope of this report to go deeply into the theory. Only a simplified derivation for the angle  $\phi$  will be given, because it gives important insights, and it can be used to derive the formula for the local Reynolds number.

The described method results in a blade geometry which is optimal, or near optimal, in terms of the  $C_p$  that can be expected. It does not mean that the designed blade is strong enough or that it is stiff enough to prevent aerodynamic instabilities, such as flutter. Also the starting torque is not a design parameter. It depends on the  $C_q$ - $\lambda$  curve of the rotor and the load characteristic if a certain rotor can be coupled to a certain load. Chapters 6 and 8 give more information on this subject.

### 5.2 Rotor parameters

The rotor geometry is determined by the following parameters:

Rotor tip radius  $R$

Number of blades  $B$

Design tip speed ratio  $\lambda_d$

Blade aerofoil as a function of the local radius  $r$

Blade chord  $c$  as a function of the local radius  $r$

Blade setting angle  $\beta$  as a function of the local radius  $r$

#### **Rotor tip radius $R$**

The rotor tip radius  $R$  is half the rotor diameter  $D$ . The electrical power  $P_{el}$  is given by formula 4.2 being:  $P_{el} = C_p * \eta_{tr} * \eta_{gen} * \frac{1}{2}\rho V^3 * \pi R^2$ .

$C_p$ ,  $\eta_{tr}$  and  $\eta_{gen}$  are not constant factors but depend very much on the matching between rotor and generator (see chapter 8).  $C_p$  decreases rapidly above the wind speed where the safety system starts to limit the rotor speed.  $\eta_{tr}$  generally decreases with decreasing power. If the generator is used for battery charging the voltage is nearly constant. For this condition  $\eta_{gen}$  decreases at increasing power, mainly because of the copper losses in the generator windings. All these effects determine the  $P_{el}$ - $V$  curve (see section 8.3 point 11) which will be unique for a certain combination of rotor, transmission, generator and safety system.

The energy generated in a certain period, e.g. a year, depends on the  $P_{el}$ - $V$  curve and on the wind speed distribution for the site where the windmill is placed (see chapter 8.3 point 12). Therefore it is not possible to determine the required rotor tip radius  $R$  simply from the required energy production per year. What can be done to get some insight is to calculate  $P_{el}$  for a relatively low wind speed for which it is expected that  $C_p$ ,  $\eta_{tr}$  and  $\eta_{gen}$  are still reasonable.



As an example  $P_{el}$  is calculated for:  $C_p = 0.4$ ,  $\eta_{tr} = 0.95$ ,  $\eta_{gen} = 0.65$ ,  $\rho = 1.2 \text{ kg/m}^3$ ,  $V = 5 \text{ m/s}$  and  $R = 1.65 \text{ m}$ , using formula 4.2. The result is that  $P_{el} = 158 \text{ W}$ .  $R$  has been chosen to be the same as in the examples in sections 5.4, 6.5 and 8.4 and the result of this rough estimation of  $P_{el}$  therefore can be compared with the real  $P_{el}$ - $V$  curve given in fig. 8.4. If the result of the calculation seems to be too high or too low compared with needs one may change  $R$  and repeat the calculation. Formula 4.2 may also be written such that  $R$  is found as a function of  $P_{el}$ .

So a certain provisional tip radius  $R$  can be found. However the availability of materials, machines, money and craftsmanship can also determine or limit the maximum value of  $R$ . In practice a certain tip radius  $R$  is first chosen in combination with the other design parameters, the generator and the safety system. The  $P_{el}$  - $V$  curve for this combination is then determined. For the calculation of the rotor geometry, it is assumed that the rotor tip radius  $R$  has been decided.

### Number of blades B

There is no exact rule to determine the number of blades  $B$ . Generally  $B$  decreases as the design tip speed ratio  $\lambda_d$  increases. Table 5.1 can be used to make an initial estimate.

$\lambda_d$	B
1	12-36
1.5	6-18
2	4-12
3	3-6
4	2-4
5-8	2-3
8-15	1-2

table 5.1 Number of blades B as a function of  $\lambda_d$

If one looks at formula 5.4 with which the chord is calculated one can see that the product of the chord  $c$  and the number of blades  $B$  must have a certain value. This means that one can take for instance three blades which have a certain chord at a certain radius or six blades with just half the chord at that radius. The following arguments may be of help to make a choice:

- 1 As the number of blades increases, the so called tip losses decrease and therefore the  $C_p$  increases with an increasing number of blades. In fig. 4.3 the effect of the number of blades on  $C_p$  has been given for  $C_d/C_l = 0$ . However the difference is only large between a one bladed and a two bladed rotor. The difference between a three bladed and a six bladed rotor is almost negligible.
- 2 If few blades are chosen the blade chord becomes large and therefore a relative large local Reynolds number is obtained (see formula 5.5). The minimum  $C_d/C_l$  values are lower for aerofoils at high rather than at low Reynolds numbers (see section 5.5) and therefore higher  $C_p$  values can be expected.

This means that  $C_p$  increases for increasing chord. The result may be that the negative influence of less blades in terms of more tip losses is compensated by the positive influence of a higher Reynolds number.

- 3 If one compares, for instance, a three bladed rotor with a certain chord with a six bladed rotor with half the chord, both having the same aerofoil, the aerofoil thickness of the six bladed rotor is also half the thickness of the three bladed one. This means that the individual blade mass (for solid blades) of the six bladed rotor is only one quarter of the blade mass of the three bladed one. The total blade mass of the six bladed rotor is half the total blade mass of the three bladed rotor. However the strength of a blade of the six bladed rotor is only one eighth of that of the three bladed rotor. The bending and torsion stiffnesses are only one sixteenth. The bending and torsion stiffness are important factors which determine flutter, which is an aerodynamic instability, and therefore the blade chord should not be too small with respect to the blade length. This is one reason why fast running rotors with a low product of  $c * B$  have only two or three blades.
- 4 Slow running rotors with a high product of  $c * B$  normally have many blades. If only a few blades were used, the blade chord becomes very large and this, in combination with the required space between rotor and tower, results in a large moment of the rotor side force around the tower centre. This may cause an instability of the safety system.
- 5 The gyroscopic moment in the rotor shaft, which is determined by the product of the rotor angular velocity, the yawing angular velocity and the moment of inertia of the rotor, fluctuates sinusoidally for one and two bladed rotors but does not fluctuate for three and more bladed rotors. Therefore one and two bladed rotors can only be used if they have a slow yawing system or if the blades are connected elastic to the hub. Windmills which are kept facing the wind by vanes, or which have a safety system which turns the head out of the wind, should preferably have three or more blades.

### **Design tip speed ratio $\lambda_d$**

Some arguments for the choice of the design tip speed ratio  $\lambda_d$  have already been given in section 4.3. Generally a high  $\lambda_d$  is chosen if the rotor is to be coupled to a generator because this reduces the gear ratio needed. However the noise generation increases strongly with increasing  $\lambda_d$ . A low  $\lambda_d$  is required if the load has a high starting torque like as in the case of a grinding mill or a piston pump. The starting torque coefficient of the rotor increases strongly with decreasing  $\lambda_d$ .

### **Blade aerofoil as a function of the local radius $r$**

The blade aerofoil can be constant or it can vary as a function of the local radius. For fast running rotors often thin aerofoils are used at the blade tip, because they have low drag/lift ratios. Thicker aerofoils are used at the blade root, because of the required bending strength. But rotors with one type of aerofoil and even with a constant chord are designed and the required strength is achieved by other means.

Slow running rotors generally are equipped with curved “flat” plates as aerofoils. The shape may change because of the structure which supports the blade. All the former CWD rotors, used for water pumping, with  $\lambda_{opt}$  between 1.5 and 2 used as an aerofoil a ten percent curved plate with tube along the centre. This aerofoil has a minimum  $C_d/C_l$  ratio of about 0.07 which is adequate for rotors with a low  $\lambda_{opt}$  (see section 4.3.3). Rotors with a higher  $\lambda_{opt}$  need aerofoils with a lower minimum  $C_d/C_l$  ratio.

Really low  $C_d/C_l$  values can only be obtained from freely supported curved plate aerofoils with limited curvature or from real aerodynamic aerofoils. It is beyond the scope of this report to evaluate different aerodynamic aerofoils. In (ref. 9.3) many aerofoils are presented. For solid wooden blades the aerofoil Gö 623 has good properties and because it has a flat lower side it can more easily be manufactured. The characteristics for this aerofoil are given in section 5.5.

### 5.3 Determination of the blade geometry

It is assumed that the rotor tip radius  $R$ , the number of blades  $B$ , the design tip speed ratio  $\lambda_d$  and the aerofoil shape have already been chosen. Only five simple formulas together with the  $C_l-\alpha$  and  $C_l-C_d$  curves of the chosen aerofoil are required for the calculation of the blade chord  $c$  and the blade setting angle  $\beta$  as a function of the local radius  $r$ . These formulas are:

#### Local design speed ratio $\lambda_{r,d}$

$$\lambda_{r,d} = \lambda_d * r / R \quad (-) \quad (5.1)$$

#### Blade setting angle $\beta$

$$\beta = \phi - \alpha \quad (^\circ) \quad (5.2)$$

#### Angle $\phi$ between the direction of the relative wind $W$ and the rotor plane

$$\phi = 2/3 \arctan 1 / \lambda_{r,d} \quad (^\circ) \quad (5.3)$$

#### Chord $c$

$$c = \frac{8 \pi r (1 - \cos\phi)}{B * C_l} \quad (m) \quad (5.4)$$

#### Local Reynolds number $Re_r$

$$Re_r = 0.667 * 10^5 * V * c * \pi (\lambda_{r,d}^2 + 4/9) \quad (-) \quad (5.5)$$

Formula 5.2 has already been derived in chapter 3 (see fig. 3.2). Derivation of formulas 5.3 and 5.4 is beyond the scope of this report. Derivation of these formulas may be found for instance in report R 1005 A (ref. 9.8).

If the rotation of the wake in the rotor plane is neglected, it is easy to derive a formula for  $\phi$  which differs only slightly from formula 5.3. This derivation gives a good insight into the rotor physics and it is also useful for the derivation of formula 5.5. Next formulas 5.1, 5.3 and 5.5 are elucidated.

### Formula 5.1

The tip speed ratio  $\lambda$  is given by formula 1.5. being:  $\lambda = \Omega * R / V$ . The local blade speed is  $\Omega * r$ , so the local speed ratio  $\lambda_r$  can be written as:

$$\lambda_r = \Omega * r / V \quad (-) \quad (5.6)$$

Combining formula 5.6 and 1.5 we get:

$$\lambda_r = \lambda * r / R \quad (-) \quad (5.7)$$

The design tip speed ratio  $\lambda_d$  is the tip speed where the power coefficient is expected to be a maximum. The blade geometry is calculated for  $\lambda_d$  so if we take  $\lambda = \lambda_d$  and  $\lambda_r = \lambda_{r,d}$ , formula 5.7 changes into:

$$\lambda_{r,d} = \lambda_d * r / R \quad (-) \quad (5.1).$$

### Formula 5.3

If the wake rotation in the rotor plane is neglected the direction of the absolute wind speed is perpendicular to the rotor plane. For extraction of the maximum power, Betz derived that the wind speed in the rotor plane must be  $2/3$  of the undisturbed wind speed  $V$  (see section 4.2). The local blade speed  $U$  at a certain radius  $r$  is  $\Omega * r$ . This results in the speed diagram of fig. 5.1.

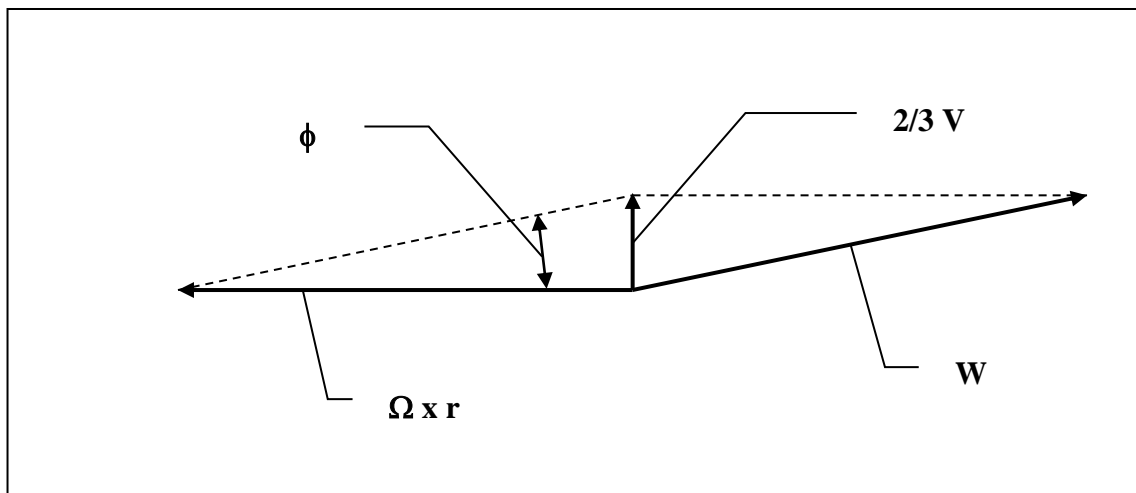


Fig. 5.1 Speed diagram for a blade cross section

It can be seen that:

$$\tan \phi = 2/3 V / \Omega * r \quad (-) \quad (5.8)$$

Combining formula 5.8 and 5.6 and  $\lambda_r = \lambda_{rd}$  we get:

$$\phi = \arctan 2/3 / \lambda_{rd} \quad (^\circ) \quad (5.9)$$

The difference between this simplified formula 5.9 and the correct formula 5.3 is that the factor 2/3 is behind the arctan. In fig. 5.2 the curves of both formulas have been plotted. It can be seen that the difference for  $\lambda_{rd} > 2$  is negligible. The simplified formula gives too large a value for the angle  $\phi$  only for small values of  $\lambda_{rd}$ .

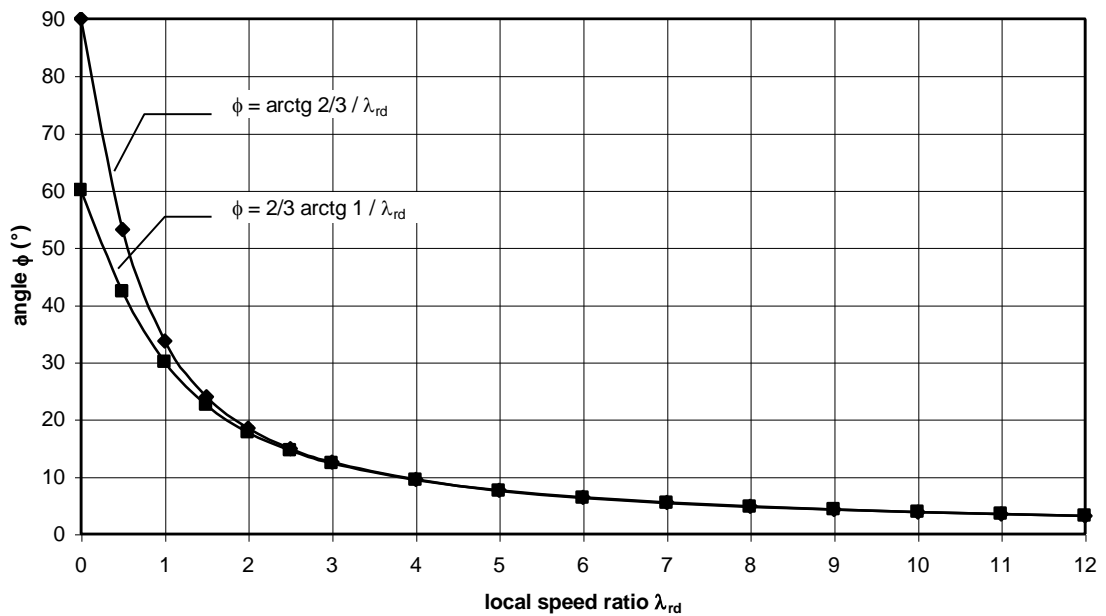


Fig. 5.2 Difference between the correct (lower line) and the simplified formulas for  $\phi$

In (ref. 9.1) the relation between  $\phi$  and  $\lambda_{rd}$  was derived as:

$$\lambda_{rd} = \frac{\sin\phi (2\cos\phi - 1)}{(1 - \cos\phi) (2\cos\phi + 1)} \quad (-) \quad (5.10)$$

It can be shown that formula 5.10 is identical to formula 5.3 which is much more simple to use and in which  $\phi$  is given explicitly.

### Formula 5.5

The Reynolds number  $R_e$  is given in formula 3.4 as:  $R_e = W * c / \gamma$

Because the wake rotation is neglected, fig. 5.1 is not quite correct, especially for low values of  $\lambda_r$ , but it is good enough for deriving a formula for the local Reynolds number  $R_{e_r}$ . Using the formula of Pythagoras in fig. 5.1 gives:

$$W = \pi (\Omega * r)^2 + (2/3 V)^2 \quad (\text{m/s}) \quad (5.11)$$

Combining formula 5.11 and 5.6 and  $\lambda_r = \lambda_{rd}$  we get:

$$W = V * \pi (\lambda_{rd}^2 + 4/9) \quad (\text{m/s}) \quad (5.12)$$

Combining formula 5.12 and 3.4:  $R_e = W * c / \gamma$ , we get for the local radius  $r$  that:

$$R_{e_r} = V * c / \gamma * \pi (\lambda_{rd}^2 + 4/9) \quad (-) \quad (5.13)$$

The kinematic viscosity  $\gamma$  for air it is about  $15 * 10^{-6}$  ( $\text{m}^2/\text{s}$ ). Substitution of this value in formula 5.13 gives:

$$R_{e_r} = 0.667 * 10^5 * V * c * \pi (\lambda_{rd}^2 + 4/9) \quad (-) \quad (5.5)$$

An appropriate wind speed  $V$  for use in this formula is the lowest wind speed for which the rotor must have good properties. Generally this will be 4 or 5 m/s.

For the calculation of the blade geometry a certain number of stations must be taken along the blade and for each station  $c$  and  $\beta$  are calculated. The distance between the stations should be smaller at the blade root than at the blade tip. Assuming that the blade aerofoil ends at about 0.1  $R$ , a good first choice is to take seven stations A to G as illustrated in fig. 5.3.

Next it is easy to construct a table in which all the calculated parameters for the different stations are given (see tables 5.2 and 5.3). The sequence of the theoretical values indicated with  $_{th}$  in the table matches the sequence of the calculation. The linearised values indicated with  $_{lin}$  are calculated afterwards.

If one starts with the geometry calculation for a certain rotor it is easy first to substitute the chosen values for  $R$ ,  $\lambda_d$ ,  $B$  and  $C_l$  or  $c$  in formulas 5.1 to 5.5 and to work with these simpler formulas. The final geometry depends on the chosen aerofoil, the lift coefficient and the linearisation of the chord and the twist. These items will be elucidated in the examples in section 5.4.

## 5.4 Examples of rotor design

Both examples given in this chapter concern fast running rotors for the generation of electricity. In the first example the lift coefficient is taken as a constant over the whole blade and it has a value for which the drag-lift ratio  $C_d/C_l$  is a minimum. If  $C_d/C_l$  is minimised, the highest  $C_{p \max}$  can be expected. In the second example the blade chord  $c$  has been kept constant. Although this blade will have a somewhat lower  $C_{p \max}$  it is much easier to manufacture especially if solid wood is used as the blade material. All other design parameters are the same for both examples.

The blade geometry of example no. 2 is identical to the blade geometry of the VIRYA-3.3, a windmill designed by Kragten Design in 1991.

### 5.4.1 Example no. 1

Initial parameters:

diameter  $D = 3.3$  m so  $R = 1.65$  m

number of blades  $B = 3$

design tip speed ratio  $\lambda_d = 5$

aerofoil Gö 623 (see section 5.5)

$C_d/C_l$  is a minimum so take  $C_l = C_{l \text{ opt}} = 0.8$

$Re_r$  is calculated for  $V = 4$  m/s

blade length  $k = 1.5$  m

Formula 5.1 with  $R = 1.65$  m and  $\lambda_d = 5$  gives:

$$\lambda_{rd} = 3.0303 * r \quad (-) \quad (5.14)$$

Formula 5.4 with  $B = 3$  and  $C_l = 0.8$  (see determination below) gives:

$$c = 10.472 * r (1 - \cos\phi) \quad (m) \quad (5.15)$$

Formula 5.5 with  $V = 4$  m/s gives:

$$Re_r = 2.667 * 10^5 * c * \pi (\lambda_{rd}^2 + 4/9) \quad (-) \quad (5.16)$$

Formula 5.2:  $\beta = \phi - \alpha$  and formula 5.3:  $\phi = 2/3 \arctan 1 / \lambda_{rd}$  stay unchanged.

The optimum lift coefficient  $C_{l \text{ opt}}$  is found as follows. For the Gö 623 aerofoil  $C_l$ - $C_d$  curves for three different Reynolds numbers are available (see fig. 5.9). The optimum lift coefficient is determined for each Reynolds number. We find the optimal  $C_l$  value there where a straight line through the origin touches the  $C_l$ - $C_d$  curve. For  $Re = 1.2 * 10^5$ , this gives a  $C_l$  of about 0.8. Also for  $Re = 2.3 * 10^5$  and  $Re = 4.2 * 10^5$  we find an optimal  $C_l$  of about 0.8. In fig. 5.8 we see that the corresponding values for  $\alpha$  are respectively  $3.5^\circ$ ,  $3.2^\circ$  and  $2.9^\circ$  for  $C_l = 0.8$ . We choose  $C_l = 0.8$  to determine formula 5.15 and later we check if the real Reynolds numbers match with the range of available curves.

The minimum  $C_d/C_l$  ratio is the reverse tangent of a line through the origin touching the  $C_l$ - $C_d$  curve. The minimum  $C_d/C_l$  ratio can be found easily for the point of intersection with the horizontal line  $C_l = 1$ . The  $C_d$  value for this point of intersection is the  $C_d/C_l$  ratio for the tangent through the origin, so for the optimum  $C_l$  value.

For  $Re = 1.2 * 10^5$  the minimum  $C_d/C_l$  ratio is 0.034.  
 For  $Re = 2.3 * 10^5$  the minimum  $C_d/C_l$  ratio is 0.027.  
 For  $Re = 4.2 * 10^5$  the minimum  $C_d/C_l$  ratio is 0.020.

The stations for which the blade geometry is calculated are shown in fig. 5.3. The results of the calculations are presented in table 5.2. For  $C_l$ ,  $c$ ,  $\alpha$ ,  $\beta$  and  $C_d/C_l$  two values are given. The first one is the theoretical value according to the calculation. The second one is obtained after linearisation of the chord which is often done to facilitate manufacture. Linearisation of the twist is required for blades made out of curved sheet, because large stresses are introduced if a curved sheet is twisted non-linear. The first value for Reynolds is the calculated value for the chosen wind speed. The second value for Reynolds is the value for the nearest curve for which data are available.

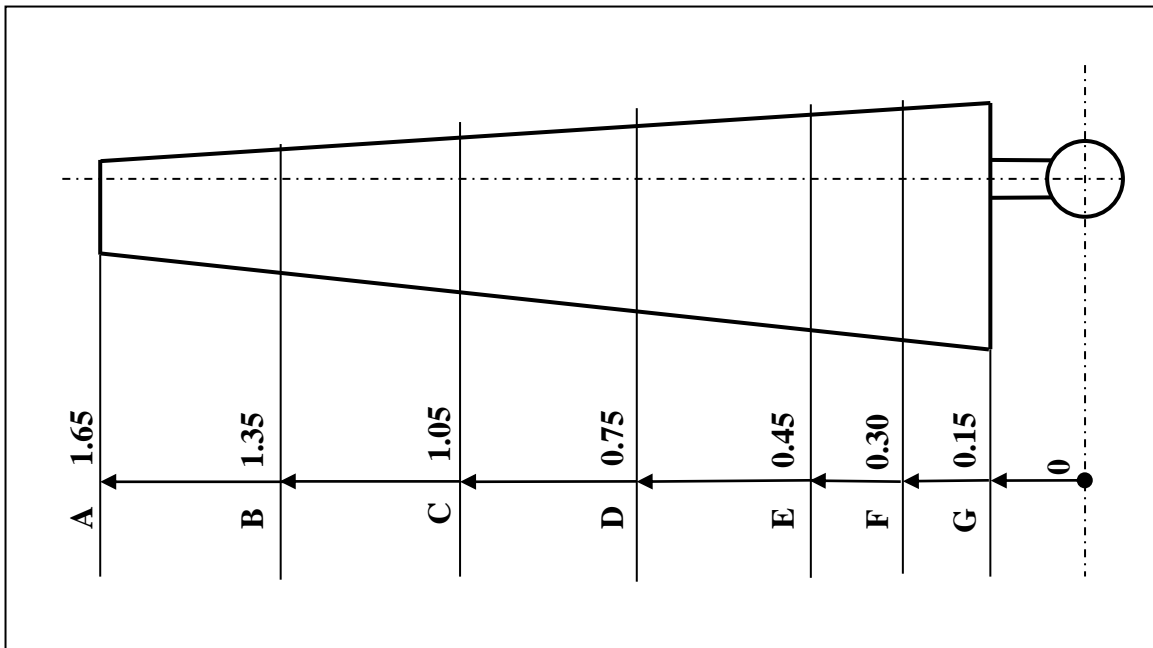


Fig. 5.3 Stations for which the blade geometry is calculated

station	r (m)	$\lambda_{rd}$ (-)	$\phi$ (°)	$C_{lth}$ (-)	$C_{lin}$ (-)	$c_{th}$ (m)	$c_{lin}$ (m)	$Re_r * 10^{-5}$ V=4m/s	$Re * 10^{-5}$ Gö623	$\alpha_{th}$ (°)	$\alpha_{lin}$ (°)	$\beta_{th}$ (°)	$\beta_{lin}$ (°)	$C_d/C_{lth}$ (-)	$C_d/C_{lin}$ (-)
A	1.65	5	7.5	0.8	0.99	0.149	0.120	2.00	2.3	3.2	5.6	4.3	3.2	0.028	0.030
B	1.35	4.091	9.2	0.8	0.80	0.180	0.180	1.99	2.3	3.2	3.2	6.0	6.0	0.028	0.028
C	1.05	3.182	11.6	0.8	0.70	0.225	0.240	1.95	2.3	3.2	2.1	8.4	9.6	0.028	0.028
D	0.75	2.273	15.8	0.8	0.79	0.298	0.300	1.88	2.3	3.2	3.1	12.6	12.7	0.028	0.028
E	0.45	1.364	24.2	0.8	0.92	0.413	0.360	1.67	1.2	3.5	5.0	20.7	19.2	0.035	0.036
F	0.3	0.909	31.8	0.8	0.97	0.472	0.390	1.42	1.2	3.5	5.7	28.3	26.1	0.035	0.037
G	0.15	0.455	43.7	0.8	0.83	0.435	0.420	0.94	1.2	3.5	3.8	40.2	39.9	0.035	0.035

table 5.2 Calculated values for a blade designed with an optimal lift coefficient



Remarks: For the calculation of the chord the angle  $\phi$  must be taken accurately (three figures after the decimal point). For the calculation of  $\beta$ , the angle  $\phi$  can be rounded off to one figure after the decimal point.

If the chord is linearised it has to be done such that the linearised chord at the outer part of the blade is as close as possible to the theoretical chord. The c-r curves are presented in fig. 5.4 before and after linearisation of the chord.

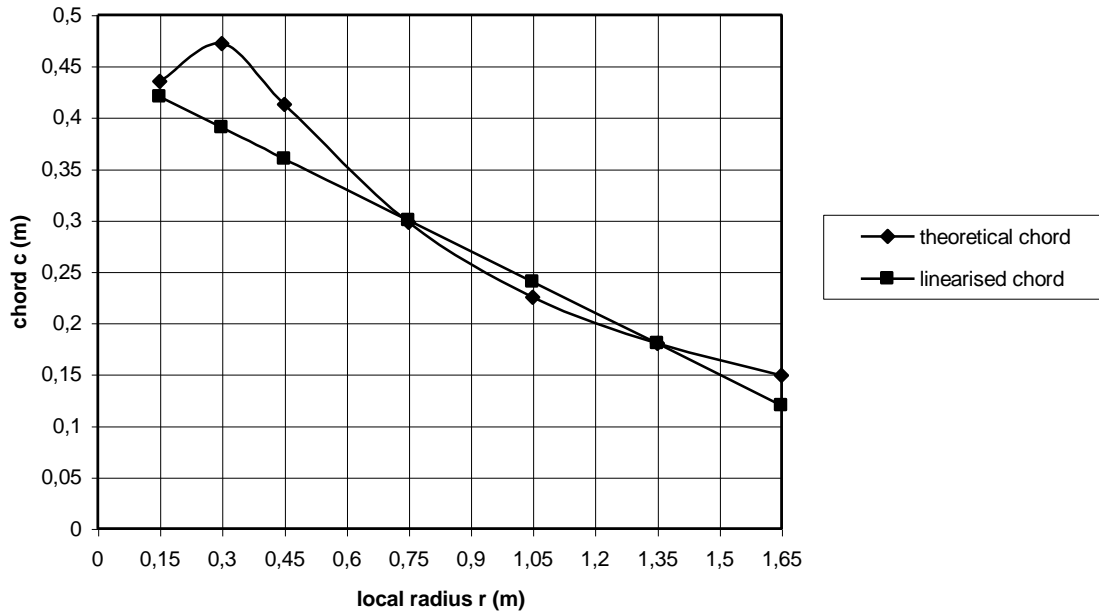


Fig. 5.4 c-r curves before and after linearisation of the chord

If the chord is changed this results in a change of  $C_1$  and therefore in changes of  $\alpha$ ,  $\beta$  and the  $C_d/C_1$  ratio. Formula 5.4 with  $B = 3$  gives:

$$C_1 = 8.378 * (1 - \cos\phi) * r / c \quad (-) \quad (5.17)$$

$C_1$  has been recalculated for the linearised chord using formula 5.17. Also  $\alpha$ ,  $\beta$  and the  $C_d/C_1$  ratio have been determined for the new  $C_1$  values. The recalculated values for a linearised chord all have as indication  $_{lin}$ . The results are placed in the right hand columns of table 5.2. If  $C_d/C_1_{lin}$  is compared with  $C_d/C_1_{th}$  it can be seen that the difference is very small so the influence of linearisation of the chord on  $C_{p \max}$  can be neglected. The  $\beta$ -r curves before and after linearisation of the chord are presented in fig. 5.5.  $C_{1 \text{ lin}}$ ,  $\alpha_{\text{lin}}$ ,  $\beta_{\text{lin}}$  and  $C_d/C_1_{\text{lin}}$  out of table 5.2 are given for linearisation of the chord only.

If  $\beta$  itself is also linearised (dotted line), this results in a blade which is, particularly near the blade root, quite different to the design theory.

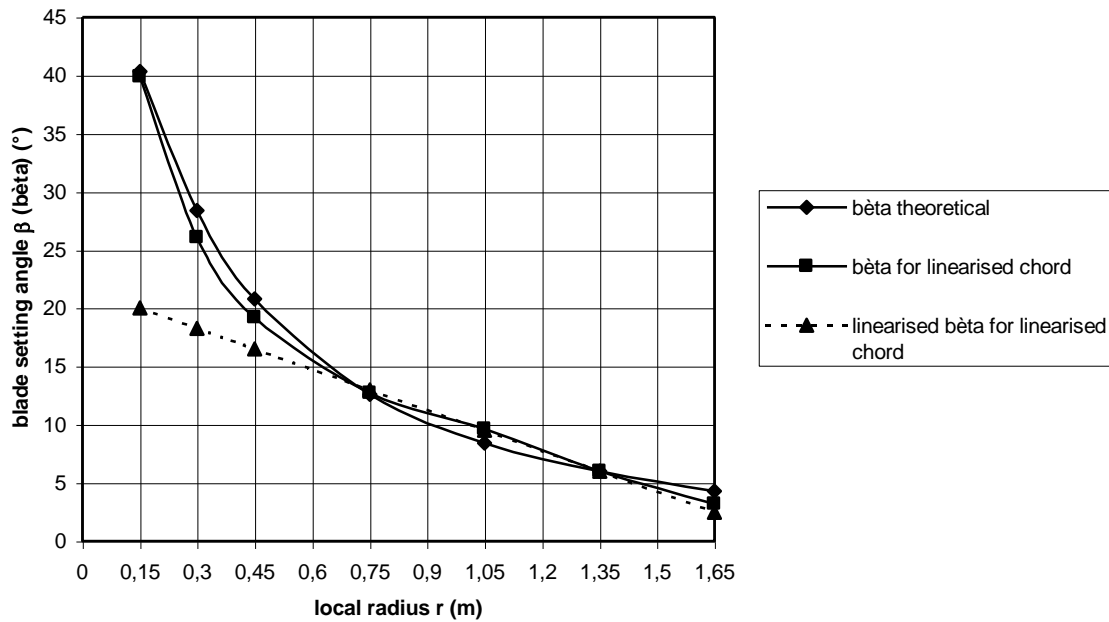


Fig. 5.5  $\beta$ - $r$  curves before and after linearisation

In table 5.2 it can be seen that the average  $C_d/C_{l \text{ lin}}$  value for the most important part of the blade, between stations A and D, is less than 0.03. For stations E to G it is about 0.036 so still very good and therefore we can take an average  $C_d/C_l$  value of 0.03 for the whole blade. Fig. 4.7 for  $B = 3$ ,  $\lambda_{\text{opt}} = 5$  and  $C_d/C_l = 0.03$  gives  $C_{p \text{ th}} = 0.455$ . Formula 6.3:  $C_{p \text{ max}} = C_{p \text{ th}} * (2Rk - k^2) / R^2$  (see chapter 6) with  $C_{p \text{ th}} = 0.455$ ,  $R = 1.65 \text{ m}$  and  $k = 1.5 \text{ m}$  gives:  $C_{p \text{ max}} = 0.45$ . This is very good for a small windmill.

#### 5.4.2 Example no. 2 (VIRYA-3.3 rotor)

For this example the rotor diameter  $D$ , the number of blades  $B$ , the design tip speed ratio  $\lambda_d$ , and the aerofoil have been taken the same as example no. 1 so:

Initial parameters:

diameter  $D = 3.3 \text{ m}$  so  $R = 1.65 \text{ m}$

number of blades  $B = 3$

design tip speed ratio  $\lambda_d = 5$

aerofoil Gö 623 (see section 5.5)

chord  $c = \text{constant}$

$Re_r$  is calculated for  $V = 4 \text{ m/s}$

blade length  $k = 1.5 \text{ m}$

However the chord is kept constant. A constant chord results in a low lift coefficient at the blade tip and a high lift coefficient at the blade root. So the  $C_d/C_l$  ratio is not optimal, but this is not essential. One can deviate from the optimal  $C_d/C_l$  ratio, as used in example no. 1, if the  $C_d/C_l$  ratio stays below a certain value. If a line is drawn on the  $C_l$ - $C_d$  graph through the origin and for example the point  $C_l = 1$ ,  $C_d = 0.05$ , all points lying on the  $C_l$ - $C_d$  curves to the left of this line will have  $C_d/C_l$  ratios smaller than 0.05 (see fig. 5.9).

For  $Re = 1.2 * 10^5$  this is the case for  $0.4 < C_1 < 1.22$ . For  $Re = 2.3 * 10^5$  this is the case for  $0.29 < C_1 < 1.26$ . If the  $C_d/C_1$  ratio is smaller than 0.05 a good  $C_p$  can still be expected for a three bladed rotor (see fig. 4.7).

The outer half of the blade generates approximately 75 % of the power because the area swept by this part of the blade is 75 % of the whole rotor area. Therefore it is necessary to ensure that this part of the blade functions well and the lift coefficient at the blade tip is not too low. A good first choice is  $C_1 = 0.6$ . With this value the blade chord at the tip is calculated using formula 5.3 and formula 5.4 as  $c = 0.199$  m. So let us take  $c = 0.2$  m. The Gö 623 aerofoil has a maximum thickness  $t$  equal to 12 % of the chord so  $t = 24$  mm which seems reasonable. The lift coefficient is now calculated for the chosen chord  $c = 0.2$  m.

Formula 5.4 with  $c = 0.2$  m and  $B = 3$  gives:

$$C_1 = 41,888 * r (1 - \cos\phi) \quad (-) \quad (5.18)$$

Formula 5.5 with  $V = 4$  m/s and  $c = 0.2$  m gives:

$$Re_r = 0.5336 * 10^5 * \pi (\lambda_r d^2 + 4/9) \quad (-) \quad (5.19)$$

Formula 5.2, 5.3 and 5.14 remain unchanged. The stations for which the blade geometry is calculated are shown in fig. 5.6. The results of the calculations are presented in table 5.3

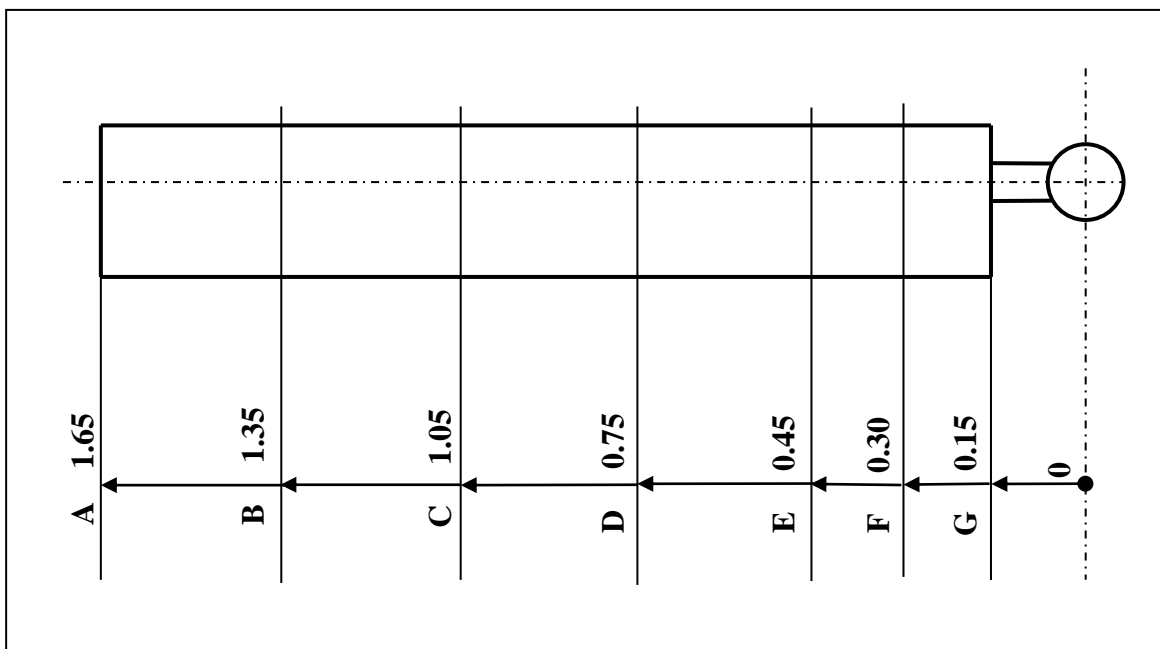


Fig. 5.6 Stations for which the VIRYA-3.3 blade geometry is calculated

station	r (m)	$\lambda_{rd}$ (-)	$\phi$ (°)	$C_{l\ th}$ (-)	$C_{l\ lin}$ (-)	$c_{lin}$ (m)	$Re_r$ * $10^{-5}$ V=4m/s	$Re$ * $10^{-5}$ Gö623	$\alpha_{th}$ (°)	$\alpha_{lin}$ (°)	$\beta_{th}$ (°)	$\beta_{lin}$ (°)	$C_d/C_{l\ th}$ (-)	$C_d/C_{l\ lin}$ (-)
A	1.65	5	7.5	0.60	0.56	0.2	2.69	2.3	0.9	0.5	6.6	7.0	0.029	0.030
B	1.35	4.091	9.2	0.72	0.71	0.2	2.11	2.3	2.3	2.2	6.9	7.0	0.028	0.028
C	1.05	3.182	11.6	0.90	0.89	0.2	1.73	2.3	4.7	4.6	6.9	7.0	0.036	0.036
D	0.75	2.273	15.8	1.19	1.15	0.2	1.26	1.2	9.6	8.8	6.2	7.0	0.046	0.044
E	0.45	1.364	24.2	1.65	0.83	0.2	0.81	1.2	-	17.2	-	7.0	-	0.340
F	0.3	0.909	31.8	1.89	-	0.2	0.60	1.2	-	24.8	-	7.0	-	-
G	0.15	0.455	43.7	1.74	-	0.2	0.43	1.2	-	36.7	-	7.0	-	-

table 5.3 Calculated values for VIRYA-3.3 blade with a constant chord

Remarks: For stations E, F and G,  $C_{l\ th}$  is higher than the maximum of the  $C_l$ - $\alpha$  curve, so no angle  $\alpha_{th}$  and therefore no angle  $\beta_{th}$  is found. The results of the calculation for stations A till D show that the angles  $\beta_{th}$  are almost constant because the increase in  $\phi$  at decreasing r is about the same as the increase in  $\alpha_{th}$ . If the angle  $\beta_{lin}$  is taken as  $7^\circ$  for the whole blade, the angle  $\alpha_{lin}$  can also be calculated for stations E, F and G. For stations F and G no values for  $C_{l\ lin}$  and  $C_d/C_{l\ lin}$  are found because the profile Gö 623 has only been measured up to  $\alpha = 17.2^\circ$  for  $Re = 1.2 * 10^5$ .

If the angle  $\beta_{lin}$  is constant for the whole blade, we get a blade with a constant chord and no twist and such a blade can be manufactured easily out of a solid wooden plank. The VIRYA-3.3 rotor is therefore easy to manufacture and the required amount of material is minimised. The value for  $C_{p\ max}$  is calculated in section 6.5.

## 5.5 Characteristics of the Gö 623 aerofoil

The Gö 623 aerofoil characteristics as used in the examples in section 5.4 are derived from report R 443 D (ref. 9.3). The original graph for the Gö 623 was very small. Using the original data new graphs with a finer grid were made which were published in report KD 463 (ref. 9.4). These graphs are presented in fig. 5.8 and fig. 5.9.

For the calculation of the starting torque coefficient (see chapter 6.3),  $C_l$ - $\alpha$  data for very large angles  $\alpha$  are required but these are not available for the Gö 623. The aerofoil shape of the Gö 623 is very similar to the NACA 4412. However the zero-line is defined differently for the aerofoils. For the Gö 623 the zero-line is the flat lower side of the aerofoil. For the NACA 4412 it is the line which connects the aerofoil leading edge with the trailing edge. The difference between these lines is about  $2^\circ$  (see fig. 5.7).

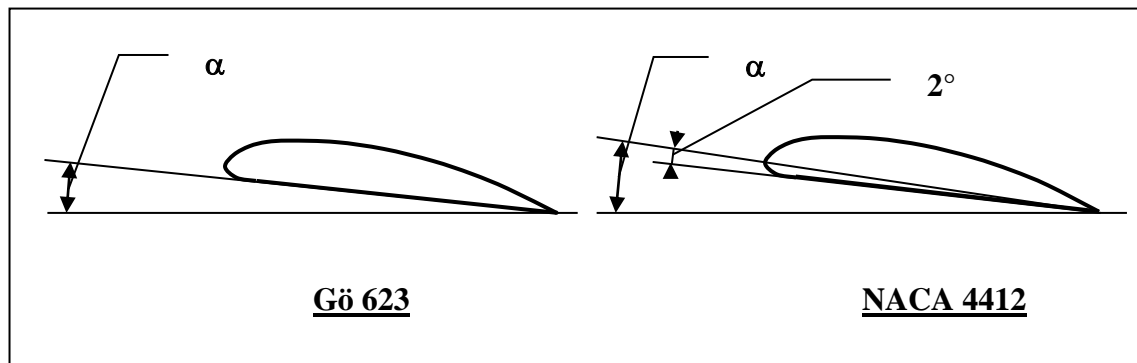


Fig. 5.7 Main differences between Gö 623 and NACA 4412 aerofoils

For the NACA 4412 aerofoil a  $C_l$ - $\alpha$  curve is available for  $-4^\circ < \alpha < 90^\circ$  and  $Re = 0.95 \cdot 10^5$  (see ref. 9.3). An estimated curve for the Gö 623 for  $16^\circ < \alpha < 90^\circ$  is derived from this NACA 4412 curve taking into account that the zero lines differ  $2^\circ$ . The result is presented in fig. 5.10.

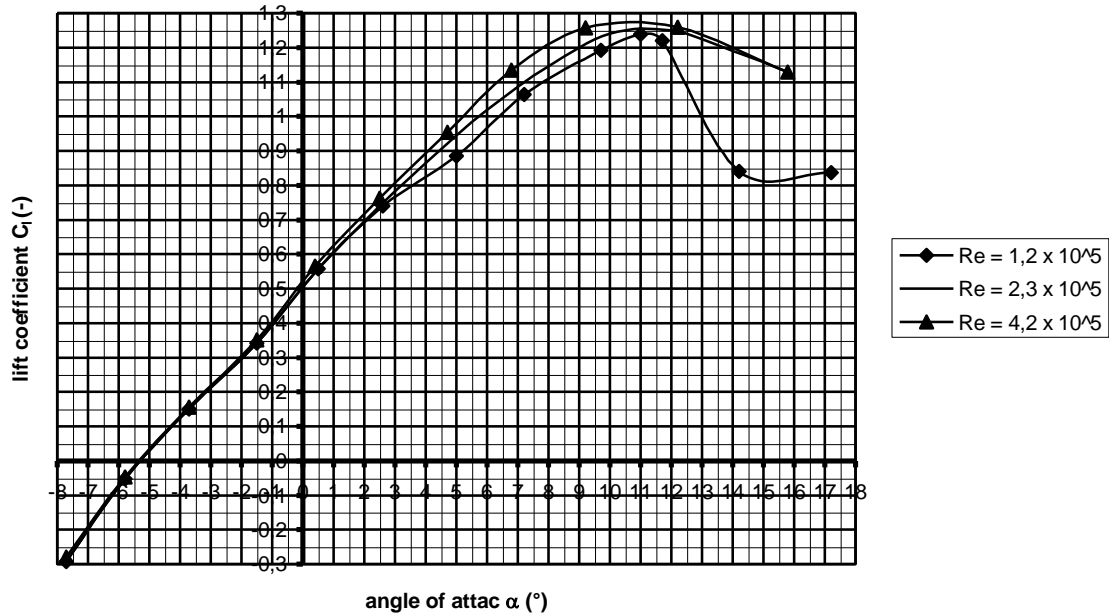


Fig. 5.8  $C_l$ - $\alpha$  curves for the Gö 623 aerofoil for three values of Reynolds

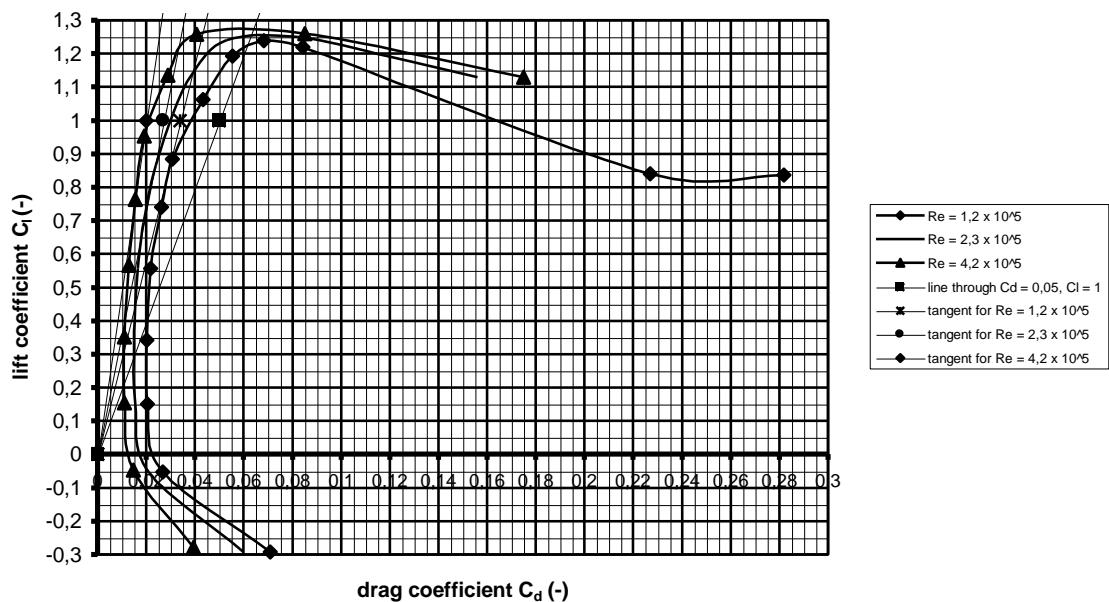


Fig. 5.9  $C_l$ - $C_d$  curves for the Gö 623 aerofoil for three values of Reynolds

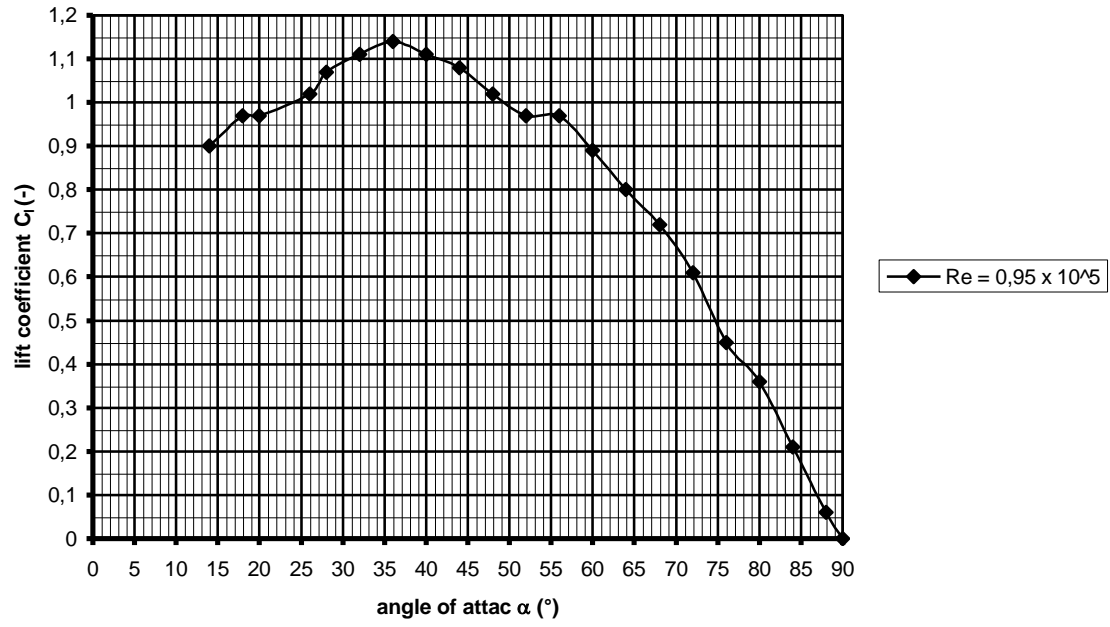


Fig. 5.10 Estimated  $C_l$ - $\alpha$  curve for the Gö 623 aerofoil for large angles  $\alpha$

The geometry of the Gö 623 aerofoil for a chord of 100 is given in fig. 5.11. The profile looks extremely thick but this is because of the difference in scale between the x-axis and the y-axis. This is done to create enough space to place the y-co-ordinates.

$x$  is the x-co-ordinate measured from the nose as a percentage of the chord.  $y_1$  is the co-ordinate of the upper side and  $y_2$  is the co-ordinate of the lower side as a percentage of the chord. The y-co-ordinates are given from the flat lower side which is the zero-line for the Gö 623 aerofoil.

Originally  $y_2 = 0.35$  for  $x = 7.5$  but in this case there is a bulge in the curve. Therefore it has been changed into  $y_2 = 0.45$ . The maximum thickness of 12 % of the chord is reached at  $x = 30$ .

If the blade is made of wood it is advised to enlarge the aerofoil thickness near the tailing edge to make it less prone to damage. The aerofoil can be modified in this case by taking  $y_1 = 2.95$  for  $x = 90$ ,  $y_1 = 1.85$  for  $x = 95$  and  $y_1 = 0.75$  for  $x = 100$ . The upper side of the aerofoil is now straight between  $x = 70$  and  $x = 100$ . It is expected that this small modification has no influence on the aerofoil characteristics.

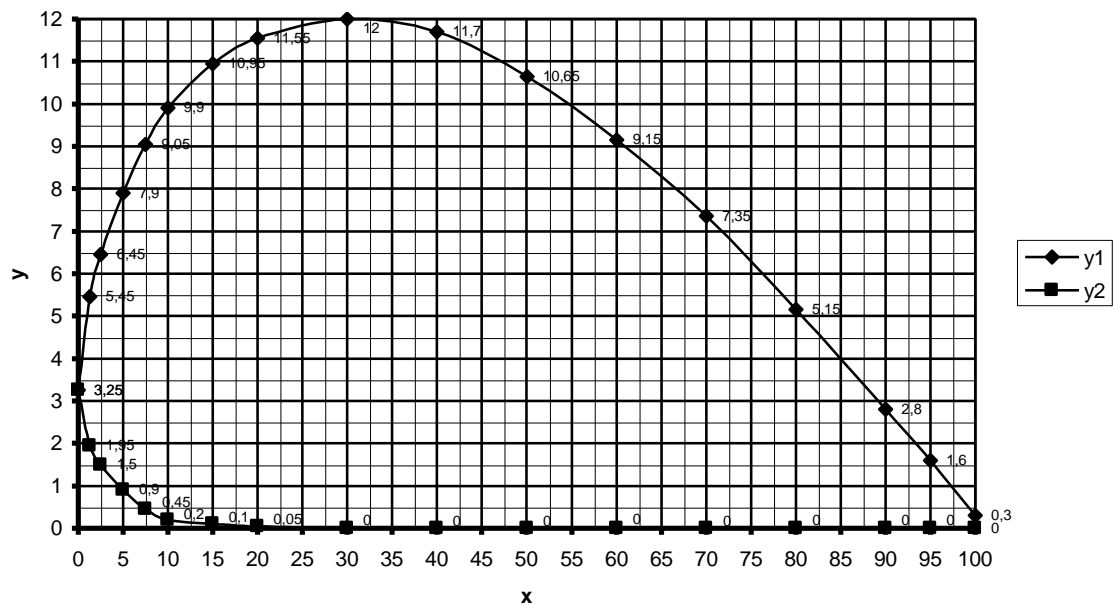


Fig. 5.11 Geometry of the Gö 623 aerofoil

## 6 Rotor characteristics

### 6.1 General

Once the rotor geometry has been determined, one often wants to know what kind of  $C_p$ - $\lambda$  and  $C_q$ - $\lambda$  curves can be expected. Different computer programs have been developed with which this is possible, but they are not generally available and the result may differ a lot from wind tunnel tests. One computer programme has been described in a TUE report: A numerical method for the determination of the performance of windmill rotors, report R 1005 A (In Dutch, ref. 9.8).

Making a scale model of the rotor and testing it in a wind tunnel is the best way, if it is tested at the correct wind speed. The wind speed should be inversely proportional to the scale factor, to obtain the correct Reynolds numbers. However wind tunnels are not available everywhere and making a scale model is a lot of work. Therefore a simple method is given which results in  $C_p$ - $\lambda$  and  $C_q$ - $\lambda$  curves which roughly correspond with measured curves.

### 6.2 Determination of $\lambda_{opt}$ , $C_{p \max}$ and $\lambda_{unl}$

Determination of  $\lambda_{opt}$

$\lambda_{opt}$  is the tip speed ratio for which one should obtain the maximum  $C_p$ . It is assumed that this is the case for the design tip speed ratio so  $\lambda_{opt} = \lambda_d$ .

Determination of  $C_{p \max}$

For each station the  $C_d/C_l$  value has been determined (see examples in section 5.4). Because approximately 75 % of the power is generated by the outer half of the blade, the average  $C_d/C_l$  value for this part of the blade is determined. Next the theoretical maximum  $C_p$  value  $C_{p \text{ th}}$  is determined using the curves presented section 4.3.3. The  $C_p$  value found in this way is too high because it is based on a blade which has the correct aerofoil from the centre of the rotor right up to the blade tip. In reality there is a disk in the middle of the rotor with radius  $R - k$  for which the blade has no aerofoil and which therefore generates no power. It is assumed that the real  $C_p$  is proportional to the ratio between the area  $A_k$  swept by a rotor blade with length  $k$  and the rotor area  $A_r$  (see fig. 6.1).



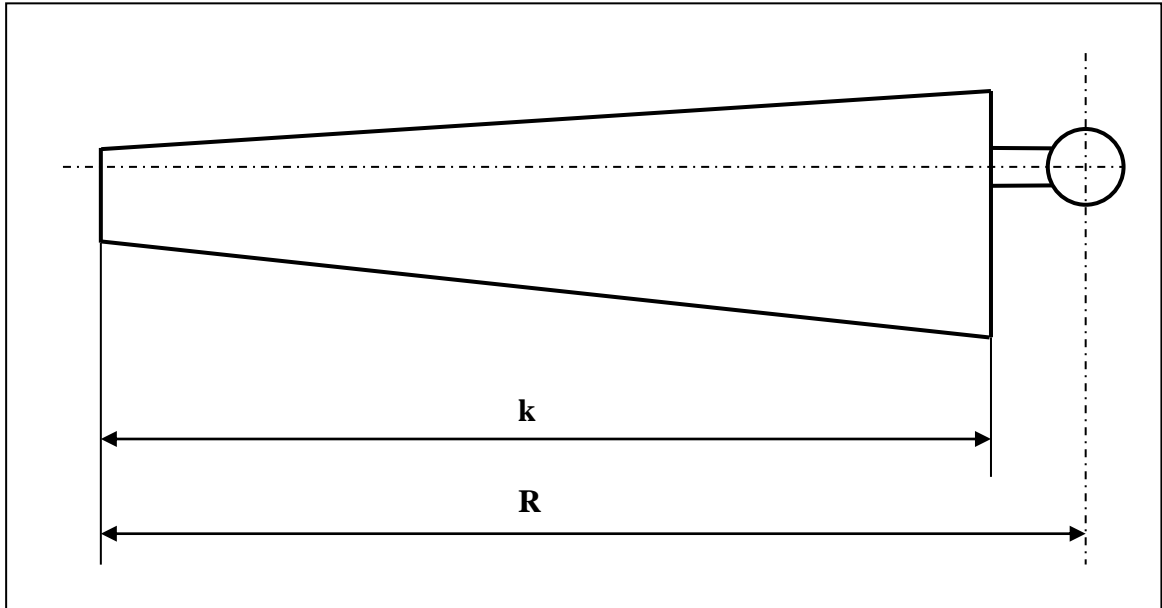


Fig. 6.1 Blade with blade length  $k$

The area  $A_k$  swept by a blade with length  $k$  is given by:

$$A_k = \pi (2Rk - k^2) \quad (\text{m}^2) \quad (6.1)$$

The rotor area  $A_r$  is given by:

$$A_r = \pi R^2 \quad (\text{m}^2) \quad (6.2)$$

So  $C_{p \max}$  is given by:

$$C_{p \max} = C_{p \text{ th}} * (2Rk - k^2) / R^2 \quad (-) \quad (6.3)$$

Determination of  $\lambda_{\text{unl}}$

For  $\lambda_{\text{unl}}$  a rule of thumb is used:

$$\lambda_{\text{unl}} = 8/5 * \lambda_{\text{opt}} \quad (-) \quad (6.4)$$

### 6.3 Determination of $C_{q \text{ start}}$

For the general determination of the starting torque coefficient  $C_{q \text{ start}}$ , the blade is divided into about six sections (see fig. 6.2).

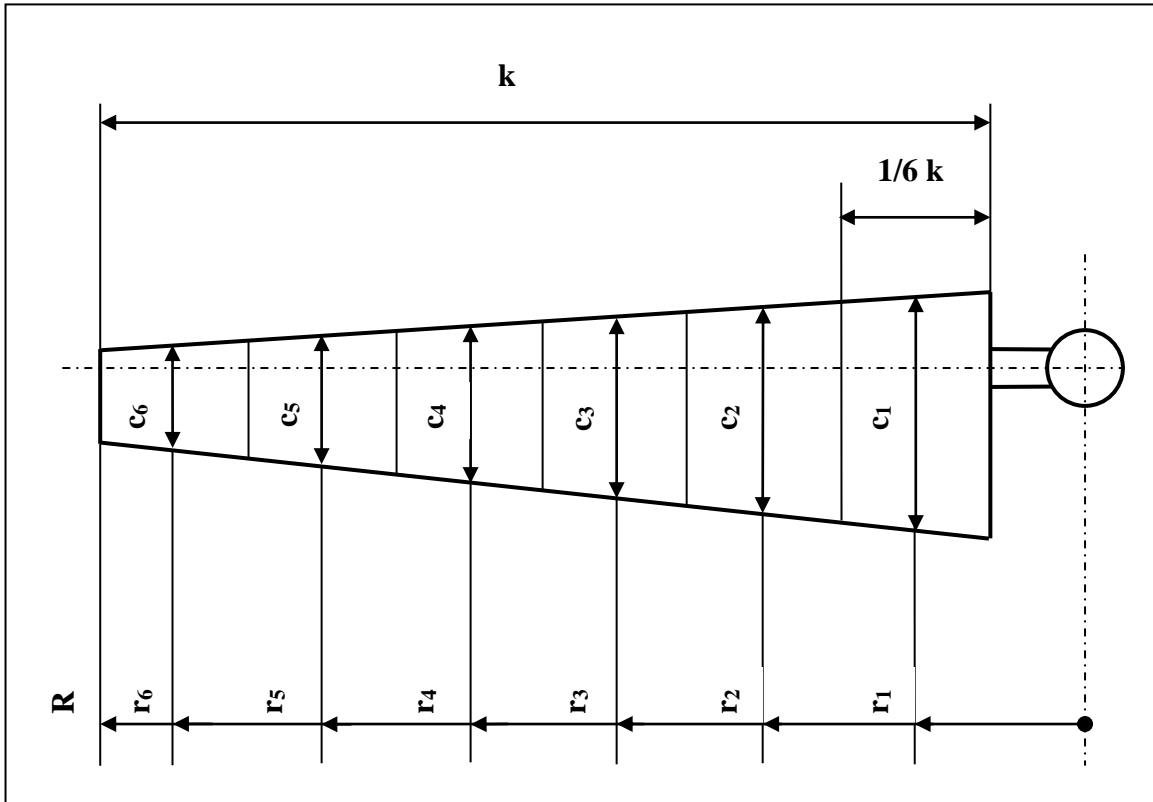


Fig. 6.2 Blade divided into six sections

For each section the average chord  $c$ , the average blade setting angle  $\beta$  and the average radius  $r$  is determined. Next the starting torque is determined for each section and the addition of the torques of all the sections multiplied by the number of blades gives the theoretical starting torque of the whole rotor. Because of losses at the blade tip and the blade root the real starting torque is about 75 % of the calculated torque.

If the blade has a constant chord and no twist (as in example no. 2 of section 5.4) the whole calculation becomes very simple because only one section having the length of the blade is required. The starting torque formulas will be derived for this condition. If the blade has a constant chord and a linear twist the same formula can be used but one has to take the average blade setting angle, that is the blade setting angle at the middle of the blade. Theoretically a small error results but this can be neglected. In fig. 6.3 the situation is given for a blade with a constant chord and a constant blade setting angle.

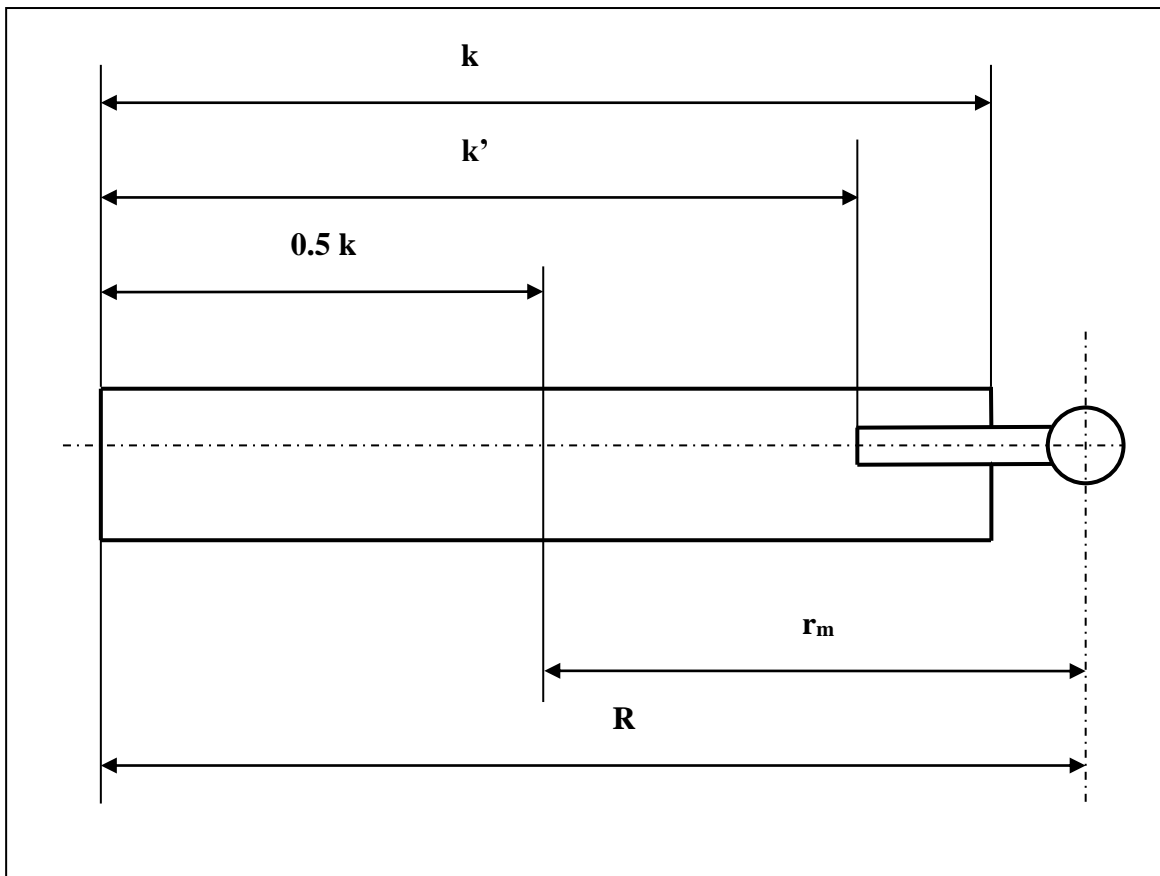


Fig. 6.3 Blade with a constant chord and no twist

For the starting condition the blade is not moving so the direction of the relative wind  $W$  is parallel to the rotor shaft. This means that  $\phi = 90^\circ$  and  $\alpha = 90^\circ - \beta$ . Because no power is extracted from the wind the relative wind speed  $W$  is the same as the undisturbed wind speed  $V$ . For these conditions the torque is caused only by the lift component  $L$  (see fig. 6.4). The resulting lift force  $L$  on the whole blade acts half way along the blade at a radius  $r_m$  (see fig. 6.3) given by:

$$r_m = R - \frac{1}{2} k \quad (\text{m}) \quad (6.5)$$

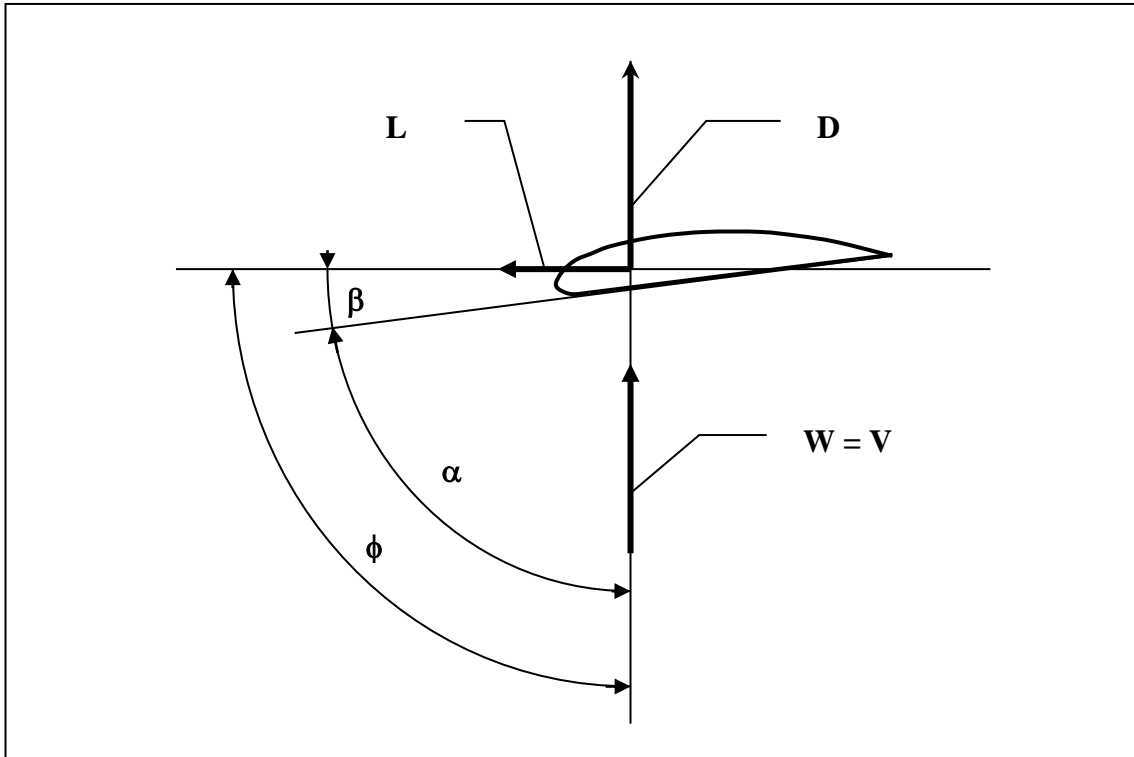


Fig. 6.4 Lift and drag on a stationary blade

The lift coefficient  $C_l$  is defined by formula 3.1. For  $W = V$  and  $b = k$  this formula can be written as:

$$L = C_l * \frac{1}{2} \rho V^2 * c * k \quad (\text{N}) \quad (6.6)$$

During starting the Reynolds number is very low and therefore we have to use the  $C_l$ - $\alpha$  curve with the lowest available Reynolds number to calculate  $C_l$ .

The theoretical starting torque of one blade  $Q_{bl \text{ th}}$  is given by:

$$Q_{bl \text{ th}} = r_m * L \quad (\text{Nm}) \quad (6.7)$$

The theoretical starting torque of the whole rotor  $Q_{rot \text{ th}}$  is given by:

$$Q_{rot \text{ th}} = B * r_m * L \quad (\text{Nm}) \quad (6.8)$$

The realistic starting torque  $Q_{start}$  is only 75 % of the theoretical starting torque so  $Q_{start}$  is given by:

$$Q_{start} = 0.75 * B * r_m * L \quad (\text{Nm}) \quad (6.9)$$

Combining formula 6.9, 6.6 and 6.5 we get:

$$Q_{start} = 0.75 * B * (R - \frac{1}{2}k) * C_l * \frac{1}{2} \rho V^2 * c * k \quad (\text{Nm}) \quad (6.10)$$

The starting torque coefficient  $C_{q \text{ start}}$  is defined as:

$$C_{q \text{ start}} = \frac{Q_{\text{start}}}{\frac{1}{2}\rho V^2 * \pi R^3} \quad (-) \quad (6.11)$$

Combining formula 6.11 and 6.10 we get:

$$C_{q \text{ start}} = \frac{0.75 * B * (R - \frac{1}{2}k) * C_l * c * k}{\pi R^3} \quad (-) \quad (6.12)$$

#### 6.4 Determination of the $C_p$ - $\lambda$ and $C_q$ - $\lambda$ curves

In sections 6.2 and 6.3 it was explained how two points lying on the  $C_p$ - $\lambda$  curve and one point lying on the  $C_q$ - $\lambda$  curve could be derived. With only these three points both curves can be estimated. This is done in four steps. Both curves are related to each other by means of formula 4.5:  $\lambda = C_p / C_q$ .

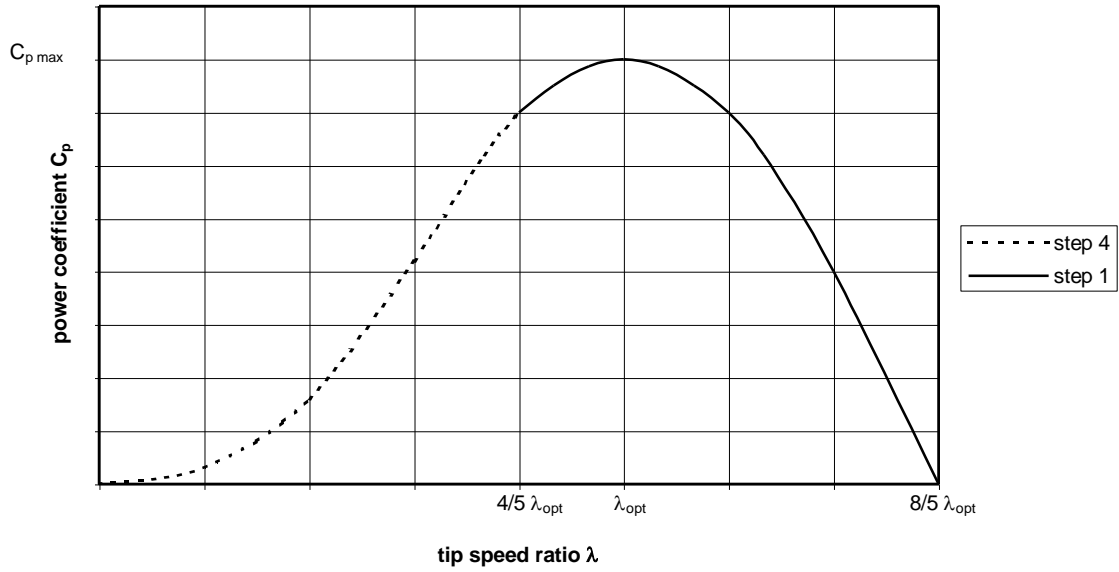
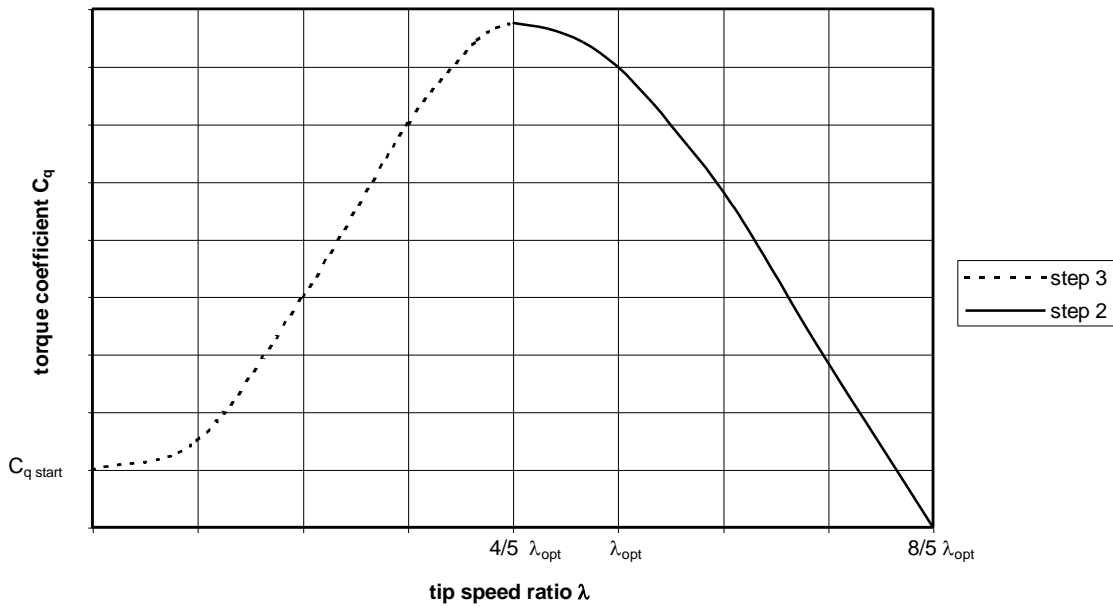
We start with the two points  $C_{p \text{ max}}, \lambda_{\text{opt}}$  and  $C_p = 0, \lambda_{\text{unl}}$ , that lie on the  $C_p$ - $\lambda$  curve. Through these two points we draw a parabola which starts at about  $\lambda = 4/5 \lambda_{\text{opt}}$  and which has a maximum at  $\lambda_{\text{opt}}$  (see fig. 6.5 black line). We read off the value for  $C_p$  for about five points on this line.

Next, using formula 4.5, we calculate the corresponding  $C_q$  values for these five points and draw the corresponding part of the  $C_q$ - $\lambda$  curve through them (see fig. 6.6 black line). The maximum  $C_q$  value normally occurs at about  $\lambda = 4/5 * \lambda_{\text{opt}}$ . The part of the  $C_q$ - $\lambda$  curve between  $\lambda = 6/5 \lambda_{\text{opt}}$  and  $\lambda_{\text{unl}}$  should be nearly a straight line. If this part of the curve is not a straight line we modify the corresponding part of the  $C_p$ - $\lambda$  curve until it is.

Next we take the calculated point for  $C_{q \text{ start}}, \lambda = 0$  and draw a horizontal line through it. Then we draw a S-shaped curve (see fig. 6.6 dotted line) which smoothly connects the point of  $C_{q \text{ start}}$  with the rest of the curve fluently and which touches the horizontal line.

Next using formula 4.5, we calculate the remaining part of the  $C_p$ - $\lambda$  curve (see fig. 6.5 dotted line) from the dotted part of the  $C_q$ - $\lambda$  curve and both curves are complete.

A more accurate method to determine the first part of the  $C_q$ - $\lambda$  curve is given in report KD 97 (ref. 9.12). This report also contains the method to determine  $C_{q \text{ start}}$  if the blade has no constant chord.

Fig. 6.5 Determination of the  $C_p$ - $\lambda$  curveFig. 6.6 Determination of the  $C_q$ - $\lambda$  curve

## 6.5 Example of rotor characteristics

The estimated  $C_p$ - $\lambda$  and  $C_q$ - $\lambda$  curves will now be derived for the VIRYA-3.3 rotor, the same rotor as used in section 5.4.2. The design tip speed ratio  $\lambda_d$  for this rotor is 5. Assume  $\lambda_{opt} = \lambda_d$ , so  $\lambda_{opt} = 5$ . The number of blades  $B = 3$ . The average  $C_d/C_l$  value is determined for the stations A to D as the most important part of the blade from table 5.3. We find  $C_d/C_l$  average = 0.04.

Next the theoretical maximum  $C_p$  coefficient is determined for a 3-bladed rotor using fig. 4.7. Only lines for  $C_d/C_l = 0.03$  and  $C_d/C_l = 0.05$  are available but by interpolation we find  $C_{p\ th} = 0.43$ . The real  $C_{p\ max}$  can be calculated with formula 6.3. The blade length  $k$  is 1.5 m. However the whole blade does not have a perfect aerodynamic aerofoil. The inner part of the blade, with a length of 0.25 m, is used for connection with the hub assembly. Although this hub assembly is positioned at the lower side of the aerofoil, it disturbs the aerofoil considerably. The effective length for the calculation of  $C_{p\ max}$  is therefore not  $k$  but  $k'$  (see fig. 6.3). For the calculation of the starting torque coefficient we can use  $k$  instead of  $k'$  because during starting the complete blade is in stall and then the influence of the hub assembly can be neglected.

Formula 6.3 with  $C_{p\ th} = 0.43$ ,  $R = 1.65$  m and  $k = k' = 1.25$  m gives:  $C_{p\ max} = 0.4$  which is a good value for a small windmill.

For the rotor designed with an optimum  $C_d/C_l$  value, as given in example no. 1 of section 5.4.1, we found that  $C_{p\ max} = 0.45$  so the difference is not large. However manufacture of this first rotor is much more difficult and much more material is required.

Formula 6.4 with  $\lambda_{opt} = 5$  gives:  $\lambda_{unl} = 8$ .

Formula 5.2 with  $\phi = 90^\circ$  and  $\beta = 7^\circ$  gives:  $\alpha = 83^\circ$ .

The aerofoil chosen is the Gö 623 and using fig. 5.10 and  $\alpha = 83^\circ$  we find  $C_l = 0.24$ .

Formula 6.12 with  $B = 3$ ,  $R = 1.65$  m,  $k = 1.5$  m,  $C_l = 0.24$  and  $c = 0.2$  m gives:  $C_{q\ start} = 0.010$ .

Next the  $C_p$ - $\lambda$  and  $C_q$ - $\lambda$  curves are determined as explained in section 6.4. The results are presented in fig. 6.7 and fig. 6.8. Note that the scale of the  $C_p$ -axis is different from the scale of the  $C_q$ -axis.

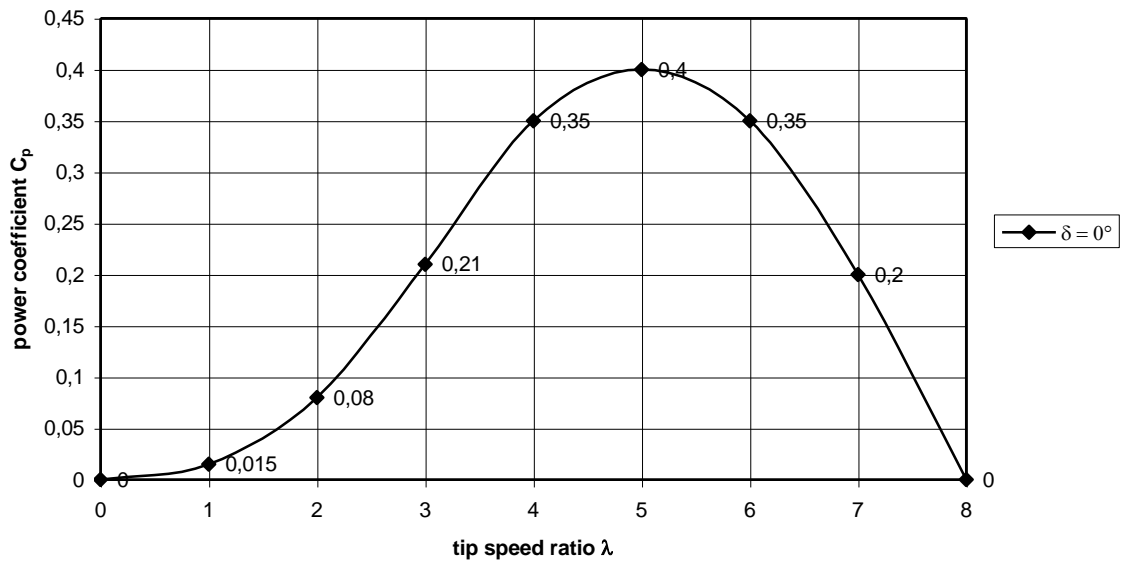


Fig. 6.7 Estimated  $C_p$ - $\lambda$  curve for the VIRYA-3.3 rotor

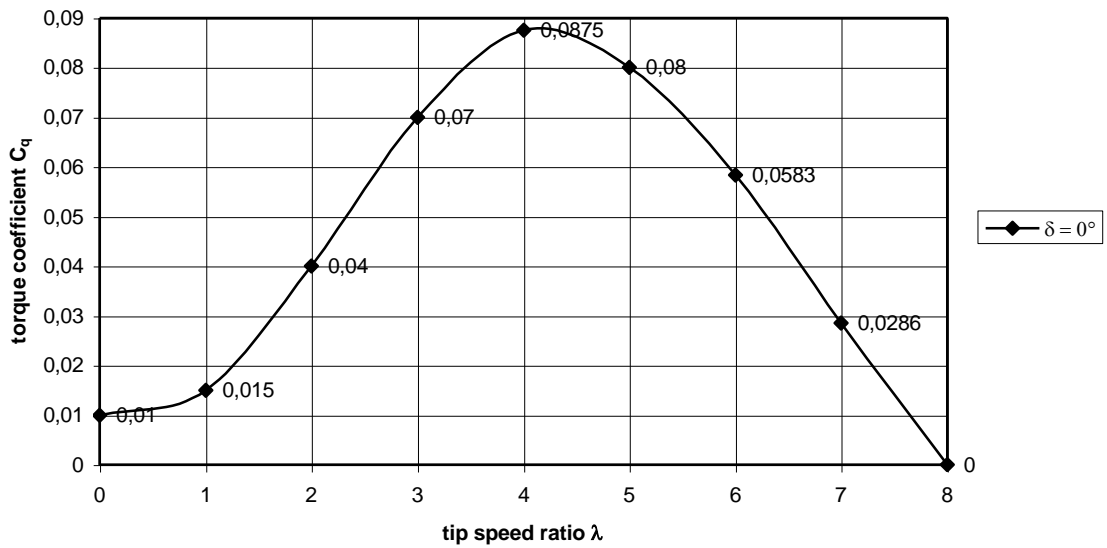


Fig. 6.8 Estimated  $C_q$ - $\lambda$  curve for the VIRYA-3.3 rotor



## 7 Rotors in yaw

### 7.1 General

The rotor characteristics as derived in chapter 6 are only valid for a rotor perpendicular to the wind. If the rotor is yawing, because of a fluctuating wind direction or because the safety system is turning the rotor out of the wind, the rotor characteristics will change. To predict how they change as a function of the yaw angle  $\delta$ , the effective component of the wind must be determined. The undisturbed wind speed before the rotor can be resolved into a component  $V\cos\delta$  perpendicular to the rotor plane and a component  $V\sin\delta$  parallel to the rotor plane (see fig. 7.1).

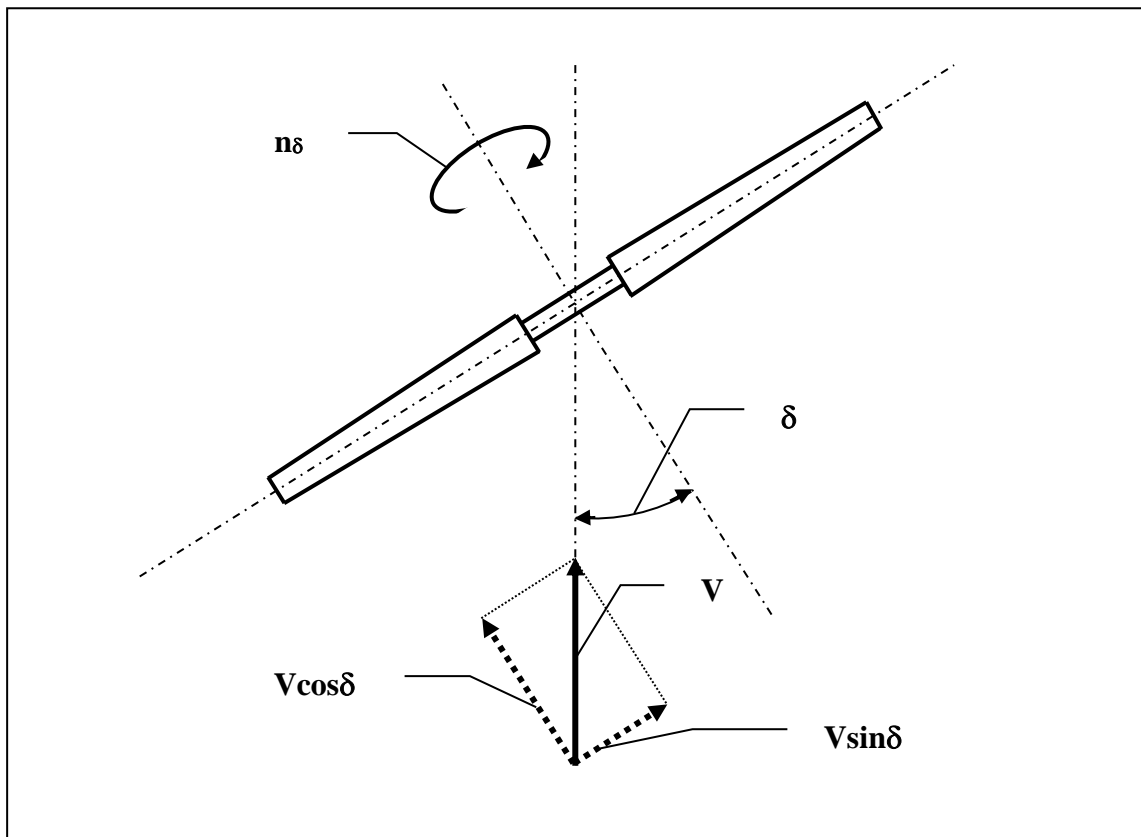


Fig. 7.1 Resolving  $V$  into components  $V\cos\delta$  and  $V\sin\delta$

Wind tunnel measurements indicate that if the component  $V\cos\delta$  is used to calculate the rotational speed, the thrust, the torque, and the power, only a small mistake is made especially in the region around the optimal tip speed ratio. The component  $V\sin\delta$  however cannot be used to calculate the side force on the rotor. The real side force is much higher than according to the calculation with  $V\sin\delta$ , especially at low values of  $\delta$ .

## 7.2 Determination of the yawing formulas

The formulas for  $n$ ,  $F_t$ ,  $Q$  and  $P$  as given in chapter 4 are now modified for yawing by using  $V \cos \delta$  instead of  $V$ .

Formula 4.8 with  $V = V \cos \delta$  gives:

$$n_{\delta} = 30 * \lambda * (V \cos \delta) / \pi R = 30 * \lambda * \cos \delta * V / \pi R \quad (\text{rpm}) \quad (7.1)$$

$$\text{Define } \lambda_{\delta} \text{ as: } \lambda_{\delta} = \lambda * \cos \delta \quad (-) \quad (7.2)$$

Combining formula 7.2 and 7.1 we get:

$$n_{\delta} = 30 * \lambda_{\delta} * V / \pi R \quad (\text{rpm}) \quad (7.3)$$

Formula 4.12 with  $V = V \cos \delta$  gives:

$$F_{t \delta} = C_t * \frac{1}{2} \rho (V \cos \delta)^2 * \pi R^2 = C_t * \cos^2 \delta * \frac{1}{2} \rho V^2 * \pi R^2 \quad (\text{N}) \quad (7.4)$$

$$\text{Define } C_{t \delta} \text{ as: } C_{t \delta} = C_t * \cos^2 \delta \quad (-) \quad (7.5)$$

Combining formula 7.5 and 7.4 we get:

$$F_{t \delta} = C_{t \delta} * \frac{1}{2} \rho V^2 * \pi R^2 \quad (\text{N}) \quad (7.6)$$

Formula 4.3 with  $V = V \cos \delta$  gives:

$$Q_{\delta} = C_q * \frac{1}{2} \rho (V \cos \delta)^2 * \pi R^3 = C_q * \cos^2 \delta * \frac{1}{2} \rho V^2 * \pi R^3 \quad (\text{Nm}) \quad (7.7)$$

$$\text{Define } C_{q \delta} \text{ as: } C_{q \delta} = C_q * \cos^2 \delta \quad (-) \quad (7.8)$$

Combining formula 7.8 and 7.7 we get:

$$Q_{\delta} = C_{q \delta} * \frac{1}{2} \rho V^2 * \pi R^3 \quad (\text{Nm}) \quad (7.9)$$

Formula 4.1 with  $V = V \cos \delta$  gives:

$$P_{\delta} = C_p * \frac{1}{2} \rho (V \cos \delta)^3 * \pi R^2 = C_p * \cos^3 \delta * \frac{1}{2} \rho V^3 * \pi R^2 \quad (\text{W}) \quad (7.10)$$

$$\text{Define } C_{p \delta} \text{ as: } C_{p \delta} = C_p * \cos^3 \delta \quad (-) \quad (7.11)$$

Combining formula 7.11 and 7.10 we get:

$$P_{\delta} = C_{p \delta} * \frac{1}{2} \rho V^3 * \pi R^2 \quad (\text{W}) \quad (7.12)$$

### 7.3 Example of yawing

Formulas 7.2, 7.8 and 7.11 can now be used to derive the  $C_{p \delta-\lambda_\delta}$  and  $C_{q \delta-\lambda_\delta}$  curves for certain values of  $\delta$ . This has been done for the VIRYA-3.3 rotor for which the rotor characteristics were given in fig. 6.7 and fig. 6.8. These curves have been produced for values of  $\delta = 15^\circ, 30^\circ, 45^\circ$  and  $60^\circ$ . It is easy to start by making a table in which all the calculated values are given (see table 7.1). The calculated values, including the values for  $\delta = 0^\circ$ , are used for the  $C_{p \delta-\lambda_\delta}$  and  $C_{q \delta-\lambda_\delta}$  curves as given in fig. 7.2 and fig. 7.3.

$\delta = 0^\circ$			$\delta = 15^\circ$			$\delta = 30^\circ$			$\delta = 45^\circ$			$\delta = 60^\circ$		
$\lambda$	$C_q$	$C_p$	$\lambda_\delta$	$C_{q \delta}$	$C_{p \delta}$	$\lambda_\delta$	$C_{q \delta}$	$C_{p \delta}$	$\lambda_\delta$	$C_{q \delta}$	$C_{p \delta}$	$\lambda_\delta$	$C_{q \delta}$	$C_{p \delta}$
0	0.01	0	0	0.0093	0	0	0.0075	0	0	0.005	0	0	0.0025	0
1	0.015	0.015	0.9659	0.0140	0.0135	0.8660	0.0113	0.0097	0.7071	0.0075	0.0053	0.5	0.0038	0.0019
2	0.04	0.08	1.9319	0.0373	0.0721	1.7321	0.03	0.0520	1.4142	0.02	0.0283	1	0.01	0.01
3	0.07	0.21	2.8978	0.0653	0.1892	2.5981	0.0525	0.1364	2.1213	0.035	0.0742	1.5	0.0175	0.0262
4	0.0875	0.35	3.8637	0.0816	0.3154	3.4641	0.0656	0.2273	2.8284	0.0438	0.1237	2	0.0219	0.0438
5	0.08	0.4	4.8296	0.0746	0.3605	4.3301	0.06	0.2598	3.5355	0.04	0.1414	2.5	0.02	0.05
6	0.0583	0.35	5.7956	0.0544	0.3154	5.1962	0.0437	0.2273	4.2426	0.0292	0.1237	3	0.0146	0.0438
7	0.0286	0.2	6.7615	0.0267	0.1802	6.0622	0.0215	0.1299	4.9497	0.0143	0.0707	3.5	0.0072	0.025
8	0	0	7.7274	0	0	6.9282	0	0	5.6569	0	0	4	0	0

table 7.1 Calculated values for  $\lambda_\delta$ ,  $C_{q \delta}$  and  $C_{p \delta}$  for the VIRYA-3.3 windmill

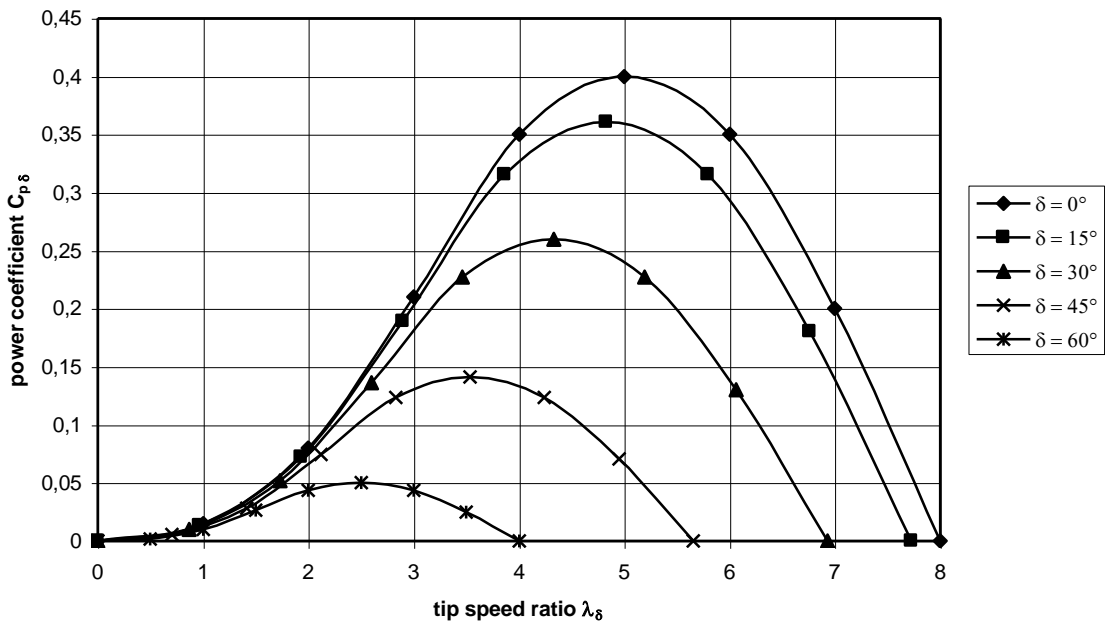


Fig. 7.2  $C_{p \delta-\lambda_\delta}$  curves for different values of  $\delta$  for the VIRYA-3.3 windmill

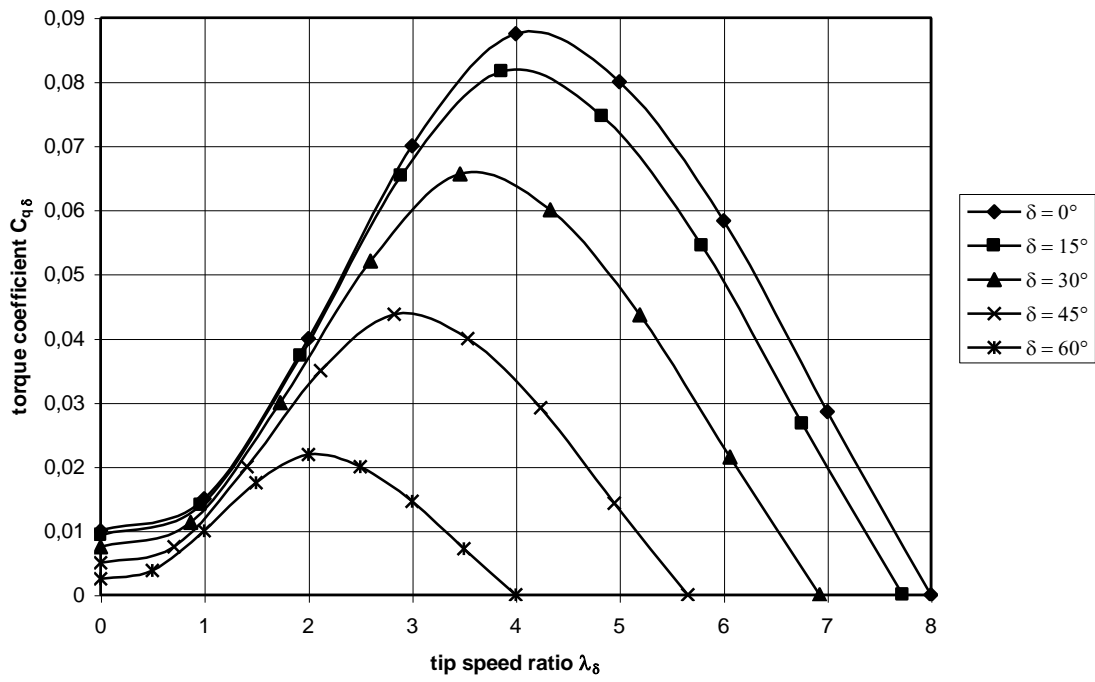


Fig. 7.3  $C_{q\delta}$   $\delta$ - $\lambda_\delta$  curves for different values of  $\delta$  for the VIRYA-3.3 windmill

## 8 Matching of windmill rotor and generator

### 8.1 General

The goal of this chapter is to give a compact method to enable the matching of a certain windmill rotor and a certain generator. Matching has to do with the extent to which the generator characteristic suits with the optimum rotor characteristic. The optimum rotor characteristic could be the P-n curve or the Q-n curve (see section 8.3 points 3 and 4) for which  $C_p$  is maximum. An advantage of using the P-n graph is that the  $P_{el}$ -n curve of the generator can be drawn on the same graph. A disadvantage is that the power is very low at very low rotational speeds and therefore the starting behaviour cannot be observed easily on the P-n graph. For observation of the starting behaviour it is better to use Q-n graphs. Both systems will be explained.

The generator characteristic can be given as measured  $P_{mech}$ -n or Q-n curves. If there is step up gearing between the generator and the windmill rotor, the gear ratio and the efficiency of the transmission have to be taken into account. The rotational speed of the generator has to be transformed to the rotational speed of the rotor shaft.

### 8.2 Design parameters

The following design parameters influence the matching between rotor and generator

- 1 The rotor diameter
- 2 The design tip speed ratio
- 3 The shape of the  $C_p$ - $\lambda$  and the  $C_q$ - $\lambda$  curve
- 4 The gear ratio of the transmission
- 5 The transmission efficiency
- 6 The type of generator, DC or AC
- 7 The type of field excitation, electro-magnet or permanent magnet
- 8 The generator size
- 9 The number of armature poles
- 10 The strength of the field density in the air gap
- 11 The method of rectification, delta or star (if used)
- 12 The number of windings per coil and the way the coils are connected to each other

Points 7 to 12 determine the open voltage at a certain rotational speed. This in combination with the battery voltage determines at which rotational speed charging starts (it is supposed that the windmill is used for battery charging).

### 8.3 Matching procedure

- 1 Determine the rotor diameter  $D$ , the design tip speed ratio  $\lambda_d$  and the blade geometry. This is described in chapter 5.
- 2 Determine the  $C_p$ - $\lambda$  and  $C_q$ - $\lambda$  curves for the chosen rotor. This could be done by using a scale model of the rotor in a wind tunnel. A simplified method for estimating these curves is given in chapter 6. About nine points have to be chosen on the selected curves and the values for  $\lambda$ ,  $C_p$ , and  $C_q$  for these points are noted in a table (see example table 8.1).

- 3 Determination of the P-n curves of the rotor. For a certain low wind speed, e.g.  $V = 3$  m/s, the chosen values for  $\lambda$  and  $C_p$  are substituted in formula 4.1 and 4.8. The calculated values for  $n$  and  $P$  are also placed in the table (see example table 8.1). This is repeated for higher wind speeds  $V = 4, 5, 6$  and  $7$  m/s. If the windmill has a safety system which turns the rotor out of the wind above for example  $V = 7$  m/s, one has to take this into account for higher wind speeds. In this case one has to use formula 7.10 and 7.1. Next the values in the table are plotted as a P-n graph (see example fig. 8.3). The line which connects points with the same wind speed is the P-n curve for that wind speed. This line has about the same shape as the  $C_p$ - $\lambda$  curve. Points with the same  $\lambda$  and the same  $C_p$  can also be connected. This line is a cubic line. The line for  $C_p = C_{p \max}$  is the optimal cubic line for the rotor. The generator curve should coincide with this line as closely as possible. The formula for the cubic lines can be found by combining formula 4.1 and 4.8 which results in:

$$P = \frac{\pi^4 * \rho * C_p * R^5 * n^3}{54000 * \lambda^3} \quad (\text{W}) \quad (8.1)$$

- 4 Determination of the Q-n curves of the rotor. Using formula 4.3 and 4.8, the procedure is identical to that described for the P-n curves. The line which connects points with the same wind speed is the Q-n curve for that wind speed. The line which connects points with the same  $C_q$  and  $\lambda$  is a quadratic line. Note that the optimal quadratic line through the points  $C_q = C_{q \text{ opt}}$ , does not go through the maxima of the Q-n curves. To observe of the starting behaviour it is enough to draw only the part of the Q-n lines that are for low values of  $\lambda$  and for low wind speeds. These lines can be compared with the Q-n curve of a generator at low rpm which is mainly due to the “sticking” torque and bearing friction. The formula for the quadratic lines can be found by combining formula 4.3 and 4.8 which results in:

$$Q = \frac{\pi^3 * \rho * C_q * R^5 * n^2}{1800 * \lambda^2} \quad (\text{Nm}) \quad (8.2)$$

- 5 Next a generator is chosen with a certain type and a certain size. The armature volume roughly determines the maximum torque level and this determines the maximum rated wind speed for a certain rotor diameter and a certain  $\lambda_{\text{opt}}$ . For small windmills it is advised that you use a standard 3-phase motor which is provided with a permanent magnet armature. All VIRYA windmills, designed by Kragten Design, use this kind of generator. If the windmill rotor is mounted directly on the generator shaft, the required shaft diameter may determine the minimum generator size.
- 6 Next a transmission system with a certain speed up gear ratio  $i$  is chosen. One should know or estimate the efficiency of the transmission  $\eta_{\text{tr}}$ . For transmissions like V-belts, the efficiency depends very much on the torque which is transmitted. For small windmills it is advised to use a slow running generator without a transmission system, so  $i = 1$  and  $\eta_{\text{tr}} = 1$ .

- 7 The chosen generator characteristic should be measured on a test rig for the rotational speed range which can be expected if it is used as a windmill generator. It is advised to measure not only for the chosen battery voltage but also for higher and lower voltages. It should also be tested unloaded and short-circuited.  $Q$ - $n$ ,  $U$ - $n$ ,  $I$ - $n$ ,  $P_{\text{mech}}$ - $n$ ,  $P_{\text{el}}$ - $n$  and  $\eta_{\text{gen}}$ - $n$  curves should be drawn for all measured conditions.
- 8 If one has chosen a speed up gear ratio, the generator curves have to be translated to the rotor shaft. This can be done using the formulas:

$$n = n_{\text{gen}} / i \quad (-) \quad (8.3)$$

$$P = P_{\text{mech}} / \eta_{\text{tr}} \quad (\text{W}) \quad (8.4)$$

$$Q = Q_{\text{gen}} * i / \eta_{\text{tr}} \quad (\text{Nm}) \quad (8.5)$$

If there is no transmission  $i = 1$  and  $\eta_{\text{tr}} = 1$  and this step is unnecessary.

- 8 Next the (translated)  $P_{\text{mech}}$ - $n$  and the  $P_{\text{el}}$ - $n$  curves of the generator are drawn on the  $P$ - $n$  graph of the windmill rotor. Optimal matching is realised if the  $P_{\text{mech}}$ - $n$  curve of the generator crosses the optimal  $P$ - $n$  curve of the windmill at two points where the wind speeds are about 4.5 and 8.5 m/s (see  $P$ - $n$  graph VIRYA-3.3 windmill fig. 8.1 line “optimal”). Matching is good if the two lines touch each other or if there is a small distance between the two lines (see line “good right”). Matching is also good if the two lines cross at wind speeds of about 3 and 9.5 m/s (see line “good left”). If the points of intersection are far apart, matching is bad (see line “bad left”). If the distance between the lines is large, matching is also bad (see line “bad right”).

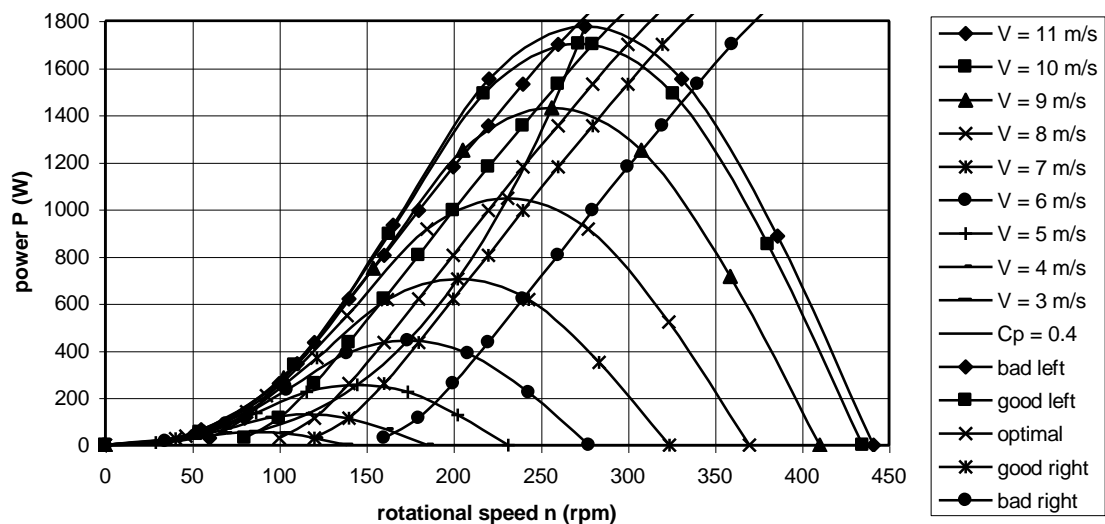


Fig. 8.1 Optimal, good and bad matching

If the matching is bad something should be changed. This may be the rotor diameter, the optimal tip speed ratio, the gear ratio, the number of windings of a coil, the way the coils are connected to each other, the method of rectification (star or delta), the number of armature poles or the strength of the magnetic field in the air gap. After modification, the matching has to be checked again. If the generator has been modified mechanically it will be necessary to measure it again. If only the winding is modified one may estimate a modified generator curve.

If the number of turns of a coil are doubled, the same generator curves will be found for the double voltage (if the total copper area of all wires in one stator groove is kept the same). The voltage halves if two coils which were connected in series are connected in parallel.

- 10 The Q-n curve of the generator is drawn on the Q-n graph of the windmill for low rotational speeds and low wind speeds. It can be seen at which wind speed the rotor Q-n curve just touches the generator curve. This is the starting wind speed. If the Q-n curve of the generator is near horizontal at low rpm, touching will take place at about zero rpm. In this case the starting wind speed can be determined by comparing the starting torque of the rotor with the sticking torque  $Q_s$  of the generator. The starting wind speed  $V_{start}$  for a gear ratio  $i = 1$  can be calculated with:

$$V_{start} = \sqrt{\frac{Q_s}{C_{q\ start} * \frac{1}{2}\rho * \pi R^3}} \quad (\text{m/s}) \quad (8.6)$$

- 11 Next the  $P_{el}$ -V curve is determined in the following way. The point of intersection of the  $P_{mech}$ -n curve of the generator with the P-n curve of the windmill for a certain wind speed, e.g.  $V = 3$  m/s, is the working point for that wind speed (see example fig. 8.3). The rotor will turn with the rpm of the working point (if the rotor is not accelerating). The electrical power  $P_{el}$  at the rpm of the working point can be found by going straight downwards, until the  $P_{el}$ -n curve is crossed. This point of intersection gives  $P_{el}$  for  $V = 3$  m/s. The same procedure is repeated for higher wind speeds. All values found for  $P_{el}$  are plotted against V in the  $P_{el}$ -V curve. The  $P_{el}$ -V curve determined in this way should be identical to the curve which one could measure if the complete windmill was placed in front of a large open wind tunnel. In literature the  $P_{el}$ -V curve is often called the P-V curve but one usually means the electrical generator power and not the mechanical power on the rotor shaft.

At a certain wind speed the safety system to limit the rotor speed and thrust will come into action. The VIRYA windmills make use of the so-called hinged side vane safety system which gradually turns the rotor out of the wind above wind speeds of about 7 m/s. The  $C_p$ - $\lambda$  curve of the rotor changes because of the safety system. The changed  $C_p$ - $\lambda$  curves of the rotor can be determined if the characteristic of the safety system is known. For a safety system which turns the rotor out of the wind one must know the  $\delta$ -V curve.  $\delta$  is the yaw angle being the angle between the wind direction and the rotor axis. In chapter 7 it is explained how  $C_p$  and  $\lambda$  change depending on the yaw angle. So for each new yaw angle, values for  $C_p$  and  $\lambda$  can be found.



The  $P_{el}$ - $V$  curve cannot be measured accurately in the field. This is because the wind speed measuring device, e.g. a cup anemometer, must be placed at a certain distance from the rotor. Depending on the wind direction, the wind speed will be measured too early or too late. The measured wind speed will also be too low if the cup anemometer is situated behind the rotor. Another problem is that real wind is never constant and that the rotor will accelerate and decelerate. So one has to select periods for which the wind speed and the rotational speed of the rotor have been constant for at least some seconds.

Sometimes  $P_{el}$ - $V$  curves are given which are based on the 10 min average wind speeds measured in the field. Such a  $P_{el}$ - $V$  curve will lie above a  $P_{el}$ - $V$  curve which is based on the momentary wind speeds, so the result is too optimistic. The difference depends on the rate of fluctuation of the wind during the measuring periods.

- 12 Finally the  $P_{el}$ - $V$  curve can be used to estimate the electric energy in kWh which will be generated during a certain period. However for this one needs the wind speed distribution for the site where the windmill will be placed. The wind speed distribution is determined from wind speed measurements over a long period. Determination of the wind speed distribution is beyond the scope of this report. The wind speed distribution gives the fraction of the time for which the wind speed was within a certain wind speed interval. Instead of the fraction one may give the number of hours per month or per year. Normally a wind speed interval has a width of 1 m/s. So the wind speed distribution gives the fraction of the time for which the wind speed is between 0 and 1 m/s and between 1 and 2 m/s and between 2 and 3 m/s and so on. The energy for each wind speed interval  $E_i$  is calculated for a certain period using the formula:

$$E_i = P_{el} * t \quad (\text{kWh}) \quad (\text{for } P_{el} \text{ in kW and } t \text{ in hours}) \quad (8.7)$$

Addition of the energy of all wind speed intervals gives the total energy  $E_{tot}$  for the chosen period.  $E_{tot}$  is given by:

$$E_{tot} = \sum E_i \quad (\text{kWh}) \quad (8.8)$$

The whole calculation is an estimation because the fluctuations of the real wind speed during a certain period will always differ from the wind speed distribution.

Example: Suppose one wants to calculate the estimated energy which will be produced during a year. A year has 8760 hours. Suppose the fraction of the wind speed interval between 4 and 5 m/s is 0.1. This means that the wind speed is between 4 and 5 m/s during 876 hours a year. Now one looks at the  $P_{el}$ - $V$  curve and determines  $P_{el}$  for a wind speed of 4.5 m/s (being the average of 4 and 5 m/s). Suppose that  $P_{el} = 120 \text{ W} = 0.12 \text{ kW}$  for  $V = 4.5 \text{ m/s}$ . Using formula 8.7 for  $P_{el} = 0.12 \text{ kW}$  and  $t = 876 \text{ h}$ , it is found that  $E_i = 105.1 \text{ kWh}$ . This is repeated for all other wind speed intervals. The total energy  $E_{tot}$  for all wind speed intervals is found using formula 8.8.

## 8.4 Example of matching

The P-n curves and the  $P_{el}$ -V curve will now be derived for the VIRYA-3.3 windmill. The blade geometry was calculated in section 5.4.2. The estimated  $C_p$ - $\lambda$  curve was determined in section 6.5. The VIRYA-3.3 windmill is provided with a 4-pole permanent magnet generator with a 3-phase winding which is rectified in delta. The windmill rotor is mounted directly to the generator shaft so the gear ratio  $i = 1$ . The generator is made from a standard asynchronous motor which is provided with a new armature with neodymium magnets.

The rpm range, used for the windmill (0 - 320 rpm), is much lower than the original motor speed (1450 rpm) and therefore the original 220/380 V winding can be used for 24 V battery charging. The measured generator characteristics are given in report KD 01, Measurements performed on the VIRYA-3.3 generator (ref. 9.9).

The VIRYA-3.3 windmill is provided with a so-called hinged side vane safety system which turns the rotor out of the wind above a certain wind speed. This safety system is described in report KD 485, Safety systems for small wind turbines which turn the rotor out of the wind at high wind speeds (ref. 9.10). An estimated  $\delta$ -V curve for the VIRYA-3.3 windmill is given in fig. 8.2.

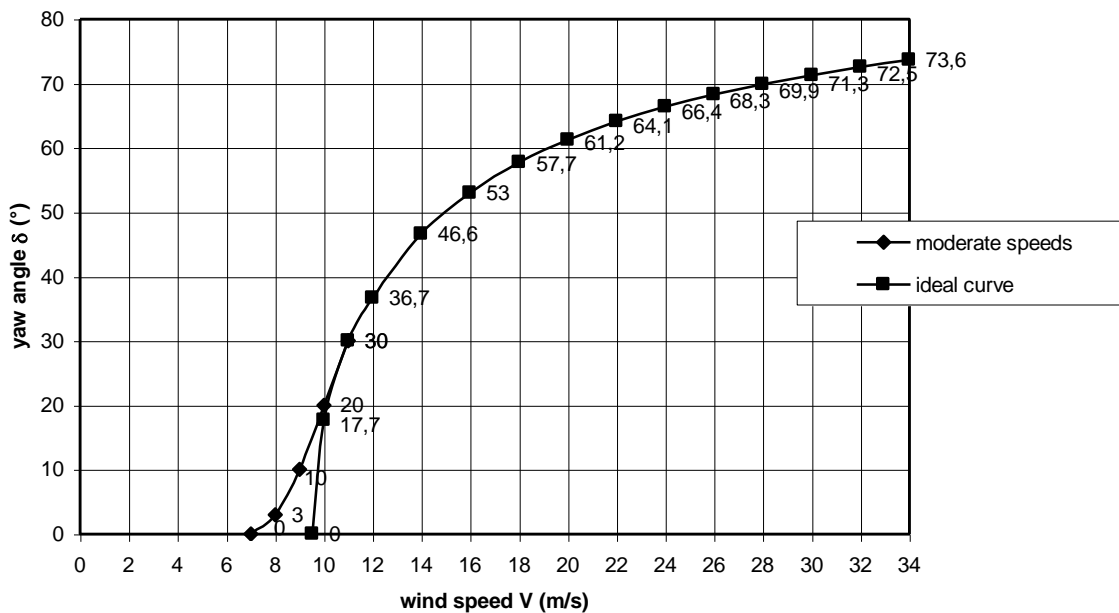


Fig. 8.2 Estimated  $\delta$ -V curve for the VIRYA-3.3 windmill

This estimated  $\delta$ -V curve is expected to follow the ideal curve  $\delta = \arccos V_{rated}/V$  for wind speeds above  $V = 11$  m/s (corresponding yaw angle  $\delta = 30^\circ$  for  $V = 11$  m/s). The theoretical  $V_{rated}$  for the given ideal  $\delta$ -V curve is 9.5263 m/s (can be calculated from the point  $V = 11$  m/s and  $\delta = 30^\circ$ ). The maximum power is reached at a wind speed of 11 m/s because the  $\delta$ -V curve does not follow the ideal curve for wind speeds below 11 m/s.  $V_{rated} = 11$  m/s is therefore the real  $V_{rated}$ .

The component of the wind speed perpendicular to the rotor plane is constant for the ideal curve. Therefore identical P-n curves will be found for wind speeds larger than  $V = 11$  m/s.

The P-n curves are determined using values for  $C_p$  and  $\lambda$  which are corrected for the effect of the yaw angle  $\delta$ . How yawing influences  $C_p$  and  $\lambda$  was explained in chapter 7. The formulas for  $n_\delta$  and  $P_\delta$  first are made more specific for the VIRYA-3.3 rotor in the following way:

Formula 7.1 with  $R = 1.65$  m gives:

$$n_\delta = 5.787 * \lambda * \cos\delta * V \quad (\text{rpm}) \quad (8.9)$$

Formula 7.10 with  $\rho = 1.2$  kg/m<sup>3</sup> and  $R = 1.65$  m gives:

$$P_\delta = 5.132 * C_p * \cos^3\delta * V^3 \quad (\text{W}) \quad (8.10)$$

The calculated values for  $n$ ,  $P$ ,  $n_\delta$  and  $P_\delta$  are given in table 8.1. The values in table 8.1 are used to produce the P-n curves given in fig. 8.3. The measured  $P_{\text{mech-n}}$  and  $P_{\text{el-n}}$  curves of the generator are also shown in fig. 8.3. The  $P_{\text{el-V}}$  curve, derived from fig. 8.3, is given in fig. 8.4.

$\lambda$	$C_p$	V = 3 m/s $\delta = 0^\circ$		V = 4 m/s $\delta = 0^\circ$		V = 5 m/s $\delta = 0^\circ$		V = 6 m/s $\delta = 0^\circ$		V = 7 m/s $\delta = 0^\circ$		V = 8 m/s $\delta = 3^\circ$		V = 9 m/s $\delta = 10^\circ$		V = 10 m/s $\delta = 20^\circ$		V = 11 m/s $\delta = 30^\circ$		
		n (rpm)	P (W)	n (rpm)	P (W)	n (rpm)	P (W)	n (rpm)	P (W)	n (rpm)	P (W)	$n_\delta$ (rpm)	$P_\delta$ (W)	$n_\delta$ (rpm)	$P_\delta$ (W)	$n_\delta$ (rpm)	$P_\delta$ (W)	$n_\delta$ (rpm)	$P_\delta$ (W)	
0	0	0	0	0	0	0	0	0	0	0	0	0	0	0	0	0	0	0	0	0
1	0.015	17.4	2.1	23.1	4.9	28.9	9.6	34.7	16.6	40.5	26.4	46.2	39.3	51.3	53.6	54.4	53.6	55.1	66.5	
2	0.08	34.7	11.1	46.3	26.3	57.9	51.3	69.4	88.7	81.0	140.8	92.5	209.3	102.6	285.9	108.8	340.7	110.3	345.9	
3	0.21	52.1	29.1	69.4	69.0	86.8	134.7	104.2	232.8	121.5	369.7	138.7	549.5	153.9	750.4	163.1	894.3	165.4	931.7	
4	0.35	69.4	48.5	92.6	115.0	115.7	224.5	138.9	388.0	162.0	616.1	184.9	915.9	205.2	1251	217.5	1490	220.5	1553	
5	0.40	86.8	55.4	115.7	131.4	144.7	256.6	173.6	443.4	202.5	704.1	231.2	1047	256.5	1429	271.9	1703	275.6	1775	
6	0.35	104.2	48.5	138.9	115.0	173.6	224.5	208.3	388.0	243.1	616.1	277.4	915.9	307.8	1251	326.3	1490	330.8	1553	
7	0.2	121.5	27.7	162.0	65.7	202.5	128.3	243.1	221.7	283.6	352.1	323.6	523.4	359.0	714.7	380.7	851.7	385.9	887.3	
8	0	138.9	0	185.2	0	231.5	0	277.8	0	324.1	0	369.9	0	410.3	0	435.0	0	441.0	0	

table 8.1 Calculated values for  $n$ ,  $P$ ,  $n_\delta$  and  $P_\delta$  as a function of  $V$ ,  $\delta$  and  $\lambda$

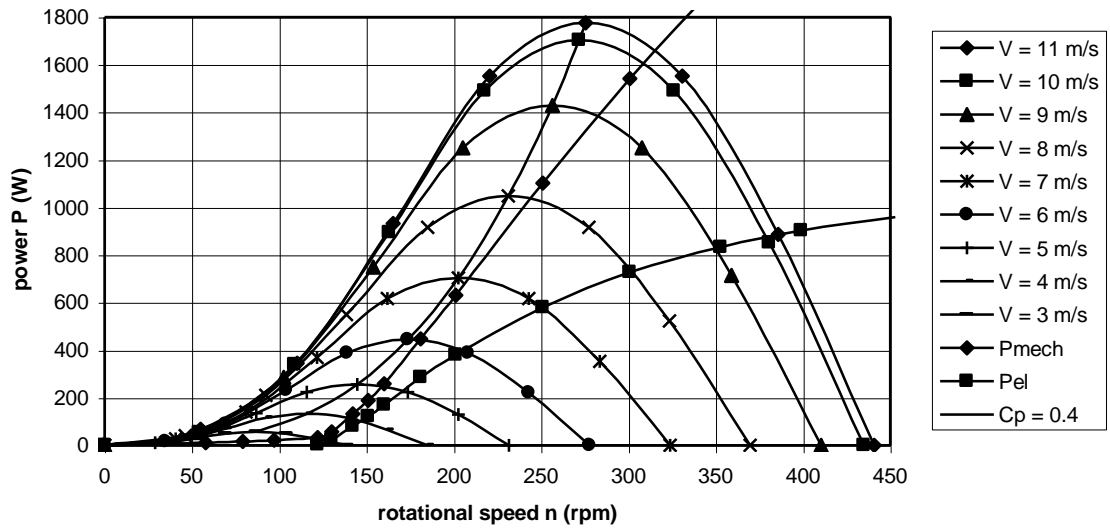


Fig. 8.3 P-n curves of the VIRYA-3.3 windmill

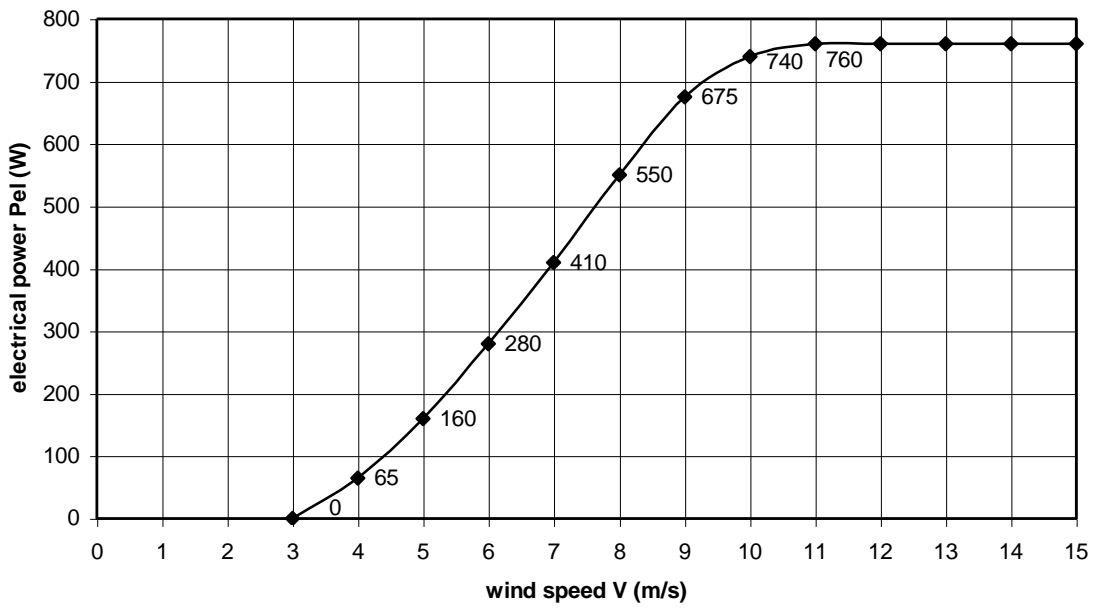


Fig. 8.4  $P_{el}$ - $V$  curve of the VIRYA-3.3 windmill

Finally the starting wind speed is calculated. From the report of the generator measurements (ref. 9.9), it can be found that the sticking torque  $Q_s = 0.6 \text{ Nm}$ .

Formula 8.6 with  $Q_s = 0.6 \text{ Nm}$ ,  $C_{q \text{ start}} = 0.01$ ,  $\rho = 1.2 \text{ kg/m}^3$  and  $R = 1.65 \text{ m}$  gives:  
 $V_{\text{start}} = 2.7 \text{ m/s}$ .

At this wind speed the rotor torque is equal to the sticking torque of the generator. However to really start, the rotor torque must be somewhat higher than the sticking torque because some torque is required to accelerate the rotor. In practice the windmill will start rotating at a wind speed of about 2.9 m/s. The cut-in wind speed  $V_{\text{cut-in}}$  is defined as the wind speed where the windmill starts to generate electricity. From fig. 8.4 it can be seen that  $V_{\text{cut-in}} = 3 \text{ m/s}$ . This means that the windmill rotor will start rotating at a wind speed just below the cut-in wind speed which is favourable because this prevents hysteresis effects.

If  $V_{\text{start}}$  is higher than  $V_{\text{cut-in}}$  hysteresis effects will occur at the wind speed interval between  $V_{\text{cut-in}}$  and  $V_{\text{start}}$ . The rotor will generate electricity only if a wind speed above  $V_{\text{start}}$  had occurred before, so if the rotor is already rotating.

The windmill rotor will stop at a wind speed which is much lower than the starting wind speed. It stops at the wind speed for which the maximum rotor torque is equal to the unloaded generator torque. For the VIRYA-3.3 windmill it has been measured that this occurs at a very low wind speed of about 1 m/s.

## 9 References

- 9.1 W.A.M. Jansen  
Horizontal axis fast running wind turbines for developing countries, CWD publication 76-1, June 1976.
- 9.2 W.A.M. Jansen en P.T. Smulders  
Rotor Design for horizontal axis windmills, CWD publication 77-1, May 1977.
- 9.3 A. Hageman  
Catalogue of Aerodynamic Characteristics of Aerofoils in the Reynolds number range  $10^4$ - $10^6$ , TUE report R 443 D, July 1980, Department of Physics, University of Technology Eindhoven.
- 9.4 A. Kragten  
The Gö 622, Gö 623, Gö 624 and Gö 625 airfoils with thickness/chord ratios of respectively 8 %, 12 %, 16 % and 20 % for use in windmill rotor blades, August 2011, free report KD 463, Engineering office Kragten Design
- 9.5 A. Kragten  
Rotor Design part 2, TUE report R 1078 D, October 1989. Department of Physics, University of Technology Eindhoven.
- 9.6 P. T. Smulders  
Rotors, TUE (has no R number), October 1991, Department of Physics, University of Technology Eindhoven.
- 9.7 A. Kragten  
Aanpassing van windmolenrotor aan generator (in Dutch), report KD 05, February 1994, Engineering office Kragten Design.
- 9.8 R. Rijs  
Een numerieke methode voor het bepalen van de prestaties van windrotoren (in Dutch). TUE report R 1005 A, June 1989, Department of Physics, University of Technology Eindhoven.
- 9.9 A. Kragten  
Measurements performed on the VIRYA-3.3 generator, report KD 01, December 1991, Engineering office Kragten Design.
- 9.10 A. Kragten  
Safety systems for small wind turbines which turn the rotor out of the wind at high wind speeds, February 2012, free report KD 485, Engineering office Kragten Design.
- 9.11 A. Kragten  
Questions and answers on a wind energy course based on report KD 35, "Rotor design and matching for horizontal axis wind turbines", in English and in Dutch, free report KD 196, May 2004, Engineering office Kragten Design.
- 9.12 A. Kragten  
Determination of  $C_q$  for low values of  $\lambda$ . Deriving the  $C_p$ - $\lambda$  and  $C_q$ - $\lambda$  curves of the VIRYA-1.8D rotor, free report KD 97, July 2002, Engineering office Kragten Design.

